HERON is jointly edited by:
STEVIN-LABORATORY of the faculty of Civil Engineering, Delft University of Technology, Delft, The Netherlands
and
TNO-INSTITUTE FOR BUILDING MATERIALS AND STRUCTURES.
Rijswijk (ZH), The Netherlands
HERON contains contributions based mainly on research work performed in these laboratories on strength of materials, structures and materials science.

ISSN 0046-7316

Secretary:
J. G. M. van Mier
Stevinweg 1
P.O. Box 5048
2600 GA Delft, The Netherlands
Tel. 0031-15-784578
Telex 38151 BUTUD NL
Fax 0031-15-786993

HERON vol. 35 1990 no. 3

Contents

YIELD LINE ANALYSIS OF POST-COLLAPSE BEHAVIOR OF THIN-WALLED STEEL MEMBERS

M. C. M. Bakker
Eindhoven University of Technology
Faculty of Architecture, Planning and Building Science

Editorial

After a period of 10 years, J. Witteveen and G. J. van Alphen have resigned as Heron Editor in Chief and Secretary respectively. They have been succeeded by A. C. W. M. Vrouwenvelder and J. G. M. van Mier, who were already members of the Editorial Board. The present board intends to continue publishing four issues a year and the scope of publications will remain unchanged.

Abstract

Thin-walled steel members are sensitive to local buckling and may fail by the development of local plastic mechanisms. In the literature many applications of (generalized) yield line theory to the analysis of these mechanisms are described. Different approaches and the validity of these approaches are discussed.

Keywords: plasticity, limit analysis, upper bound theory, yield line theory, generalized yield line, yield surface, mechanism.

Preface

The work reported in this paper is part of the research project "Web crippling of cold-formed steel members", which is performed at the Eindhoven University of Technology, in cooperation with Delft University of Technology, TNO-IBBC and Cornell University (USA). Web crippling is the localized instability failure of the web of a cold-formed steel flexural member caused by the application of a concentrated load on the member. This paper was written to provide the necessary background information for the modeling of the web crippling behavior by yield line methods. These methods, as described in this paper, are not specifically related to the web crippling problem, but are of general interest for the analysis of thin-walled steel structures. The application of the yield line methods described in this paper to the web crippling problem will be given in a Ph.D. thesis on web crippling.

Yield line analysis of post-collapse behavior of thin-walled steel members

1 Introduction

The purpose of this report is to describe yield line methods which can be used for the analysis of the post-yield or post-collapse load-deformation behavior of thin-walled steel members. This post-collapse behavior is important because it provides insight into the ductility of the structure, and it can be used to calculate a rough estimate of the failure load of the member.

To explain how the post-collapse behavior of a member can be used to estimate the failure load, the load-deformation behavior of a thin-walled steel member subjected to an increasing load will be considered. As long as the load and deformations are small the steel wil behave elastically and the load-deformation behavior of the structure can be calculated from the theory of elasticity. This behavior can be represented as an elastic loading curve in a load-deformation diagram (see Fig. 1). With increasing load, the steel will start to yield locally. The areas in which yielding occurs will expand until a failure mechanism develops. The final process of collapse can be analyzed by applying rigid-plastic theory to this (yield line) mechanism. The post-collapse behavior of the member can be represented as a plastic unloading curve in the load-deformation diagram. The failure load of the member can be estimated by determining the point of intersection of the elastic loading and the plastic unloading curves. This is called the "cut-off" strength. In principle, this estimate will be an upper bound for the exact failure load because the actual load-deformation curve will start to deviate from the elastic

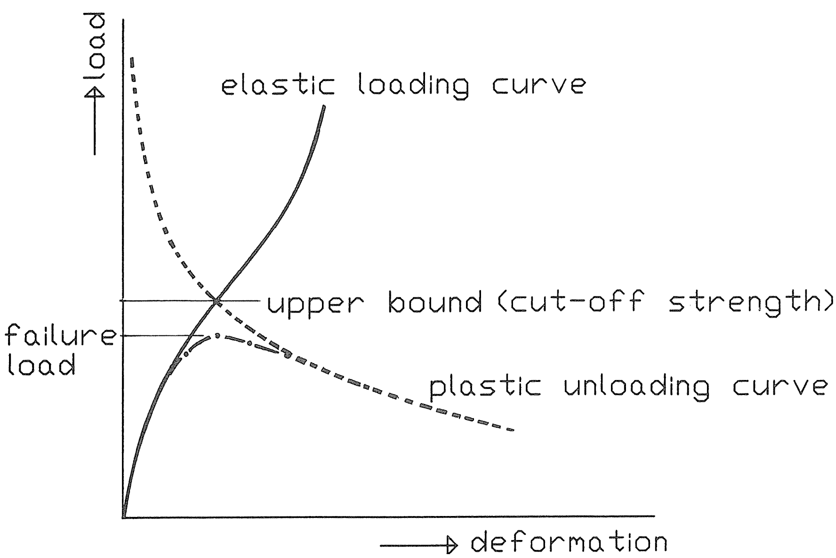

Fig. 1. A general load-deformation diagram.

loading curve at first yield and will coincide with the plastic unloading curve only after the formation of a complete failure mechanism, that is, after failure. This failure load prediction may be accurate enough for engineering purposes and provides an insight into the parameters determining the failure load of the member. A good example of an application of the method explained above can be found in a paper by Narayanan and Chow [14].

As mentioned before, the purpose of this paper is to discuss yield line methods for the analysis of the load-deformation behavior of thin-walled steel members. All these methods are derived from classical yield line theory, which is an upper bound limit analysis technique for the calculation of limit loads of reinforced concrete plates loaded by forces perpendicular to the plate. This paper therefore starts with a short summary of the theorems of limit analysis and classical yield line theory in chapters 2 and 3, respectively.

The yield line theory used to analyze the load-deformation behavior of thin-walled steel members is called generalized yield line theory. In order to adapt classical yield line theory for this purpose two points have to be considered. First, limit analysis was developed to calculate limit loads, not to calculate load-deformation behavior of structures. Second, an appropriate yield criterion has to be formulated. These two aspects of generalized yield line theory are discussed in chapter 4. Also in chapter 4, the expressions for the fully plastic moment, normal force and shear force in a yield line are derived based on the Von Mises yield surface, because the correct expressions seem not to be generally known. Finally, the limitations on the validity of generalized yield line theory are described.

In the literature many applications of generalized yield line theory are described. An extensive summary of rigid-plastic formulations for plates, including yield line formulations, was given by Dean [4]. Roughly speaking, the generalized yield line formulations can be divided into the same methods as used in classical yield line theory, namely work methods and equilibrium methods. However, in generalized yield line theory these methods are not always strictly followed; often a more or less intuitive approach is used. In chapters 5, 6 and 7, the work methods, equilibrium methods and intuitive methods are explained, respectively. In chapter 8 some aspects of yield line theory are discussed. These aspects include moving yield lines, curved yield lines and the determination of yield line patterns.

In chapter 9, the most important characteristics of the generalized yield line theory are summarized. Most of these characteristics were described in the literature already, but scattered over many references.

2 Limit analysis

Limit analysis is concerned with the determination of the limit state of incipient unrestrained plastic flow in a structure. There are two different approaches to calculate limit loads, namely a static or lower bound approach and a kinematic or upper bound approach.

In the static approach one tries to find a statically admissible stress field throughout the structure. This stress field has to satisfy the local equilibrium equations, the stress boundary conditions and the yield inequality. The yield inequality requires that at no point in the structure, the reference stress exceeds the yield strength. According to the static or lower bound theorem of limit analysis, a load corresponding to any statically admissible stress field is smaller than or at most equal to the exact limit load.
In the kinematic approach one tries to define a kinematically admissible mechanism, such as a yield line mechanism, and estimates the limit load by equating the rate of energy dissipated in plastic flow to the rate of work done by the external forces. According to the kinematic or upper bound theorem of limit analysis, a load corresponding to any kinematically admissible mechanism is larger than or at least equal to the limit load.
Combining the two theorems of limit analysis, it can easily be seen that a load corresponding simultaneously to a statically admissible stress field and a kinematically admissible mechanism is equal to the exact limit load. This will be called a complete solution.
Because this paper concentrates on upper bound limit analysis, the procedure for a general upper bound analysis will be discussed in more detail. Upper bound limit analysis consists of the following steps:

1. Choose a velocity field describing a kinematically admissible mechanism.
2. Determine the (generalized) strain rates.
3. Determine the corresponding (generalized) stresses by using a yield surface and applying the normality rule.
4. Calculate an upper bound for the limit load by equating the internal rate of energy dissipation to the rate of external work by the applied forces.

3 Classical yield line theory

Classical yield line theory is an upper bound limit analysis technique for determining the ultimate load of reinforced concrete slabs loaded by forces perpendicular to the slab. An extensive discussion of this method was given by Jones and Wood [7]. In the past, it was thought that yield line theory was not fully consistent with limit analysis, because of the different yield conditions used in these two theories. Braestrup [2] however showed that the yield conditions used in classical yield line theory correspond to a yield surface called the upper yield surface (see section 3.2), which satisfies all the requirements of limit analysis.
As noted in chapter 2, upper bound limit analysis starts with the choice of a velocity field. In classical yield line theory a special velocity field which is not continuously differentiable is chosen, resulting in a discontinuous strain rate field (see Appendix B, section B.1).

3.1 *Work and equilibrium method*

In the classical yield line theory an upper bound for the limit load can be calculated by two different methods, namely the work and the equilibrium methods. The work method is based on the principle of virtual work where the work performed by the external forces due to a virtual displacement is equated to the energy dissipated in the yield lines. In the equilibrium method the equilibrium of each individual plate segment of the yield line pattern is considered. It was proven (Jones and Wood, [7]) that the equilibrium method is actually the virtual work method presented in another form. The equilibrium method should not be confused with the equilibrium methods in lower bound limit analysis. In the yield line equilibrium method only the equilibrium of the rigid plate segments is satisfied. In these segments local equilibrium may still be violated as may the yield condition.

3.2 *Conditions for a complete solution*

In order to derive an important condition for finding a complete solution in yield line theory, first the so-called upper yield surface (Braestrup, [2]) will be defined. For this the concept of a supporting plane will be used. A supporting plane of the yield surface is a plane through a point on the yield surface such that the yield surface lies entirely on one side of the plane. The convexity condition of a yield surface requires that there exists at least one supporting plane for every point on the yield surface. The upper yield surface is the surface enveloped by the supporting planes of the yield surface normal to any possible strain rate tensor in the yield lines. This can be illustrated for the Von Mises yield condition for (thin) plates subjected to bending expressed in the plane moments m_{nn}, m_{ss} and m_{ns} (defined in a x_n-x_s-x_z coordinate system with x_z being the coordinate axis perpendicular to the plane of the plate):

$$m_{nn}^2 - m_{nn} \cdot m_{ss} + m_{ss}^2 + 3 \cdot m_{ns}^2 - m_0^2 = 0, \qquad (3.1)$$

where $m_0 = 1/4 \cdot t_p^2 \cdot f_y$. The intersection of this yield surface with the plane $m_{ns} = 0$ is shown in Fig. 2 together with the corresponding upper yield surface.

A necessary, but not sufficient condition for obtaining the complete solution is that the state of stress in a point lying on the intersection of two or more yield lines does not violate the yield condition. The normality condition requires that the strain rate tensor in any point of a yield line is normal to a supporting plane through the corresponding stress point on the yield surface. For a point on the intersection of two or more yield lines the stress point should be on the intersection of the supporting planes of the yield surface normal to the strain rate tensors in the yield lines. But the stress point must also lie on the actual yield surface. Braestrup [2] therefore formulated the following two theorems:

1. "A solution involving yield lines can only be correct if the points on the upper yield surface, corresponding to the yield sections, lie on the actual yield surface."
2. "The smallest upper bound which may be found by yield line theory is the exact solution corresponding to the upper yield surface."

Thus if the actual yield surface of the plate is different from the upper yield surface, the exact limit load of the plate cannot be determined from yield line theory.

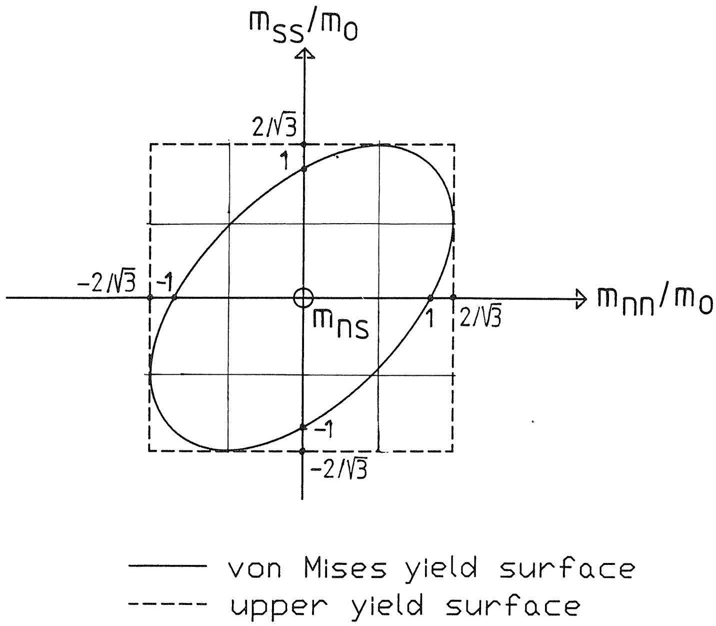

Fig. 2. Von Mises yield surface and the corresponding upper field surface.

In classical yield line theory of concrete slabs, the yield surface corresponds to the upper yield surface and therefore the complete solution can, in theory, be found by refining the yield line pattern. However, the condition that the state of stress at the intersection of yield lines must satisfy the yield condition, imposes restrictions on the angles of intersection of the yield lines. For instance, in the limit analysis of reinforced concrete slabs with isotropic reinforcement, it can be proven that positive and negative yield lines (that is yield lines with positive and negative bending moments, respectively) should intersect at angles of 90°.

4 Generalized yield line theory

In order to generalize the classical yield line theory to the analysis of the load-deformation behavior of thin walled steel members the following two points have to be considered:

1. The use of upper bound limit analysis for non-linear load-deformation behavior.
2. An appropriate yield criterion. Frequently membrane stresses will develop during the deformation of a thin-walled steel member, thus the yield criterion should account for the influence of normal and in-plane shear forces.

First these two aspects of generalized yield line theory are discussed. Then the expressions for the fully plastic moment, normal force and shear force in generalized yield line theory are derived based on the Von Mises yield surface. The corresponding interaction formulas are given in Appendix A. Finally the limitations of the validity of generalized yield line theory are discussed.

4.1 *Analysis of geometric non-linear load-deformation behavior*

Upper bound limit analysis is a technique used to calculate an upper bound for the limit load of an undeformed structure. The same technique can be used to analyse the geometrically non-linear load-deformation behavior of a structure. This is done by calculating a series of limit loads. Each calculation is based on a geometrical configuration of the structure differing from the previous one by a small amount corresponding to the collapse mode of the previous stage.
It must be noted that the exact load-deformation curve of a structure can only be determined if the complete solution at every deformation stage is known. If the complete solution is not known, only an upper bound for the limit load at each geometrical configuration can be calculated. An upper bound for the load-deformation behavior of the structure cannot be calculated. This is due to the fact that the deformation mode which is assumed in an arbitrary mechanism may never be attained in the actual mechanism (see Fig. 3). In general it is impossible to calculate the complete solution at every deformation state. Therefore it is important to remember that although an upper bound limit analysis technique is used, the analysis does not result in an upper bound for

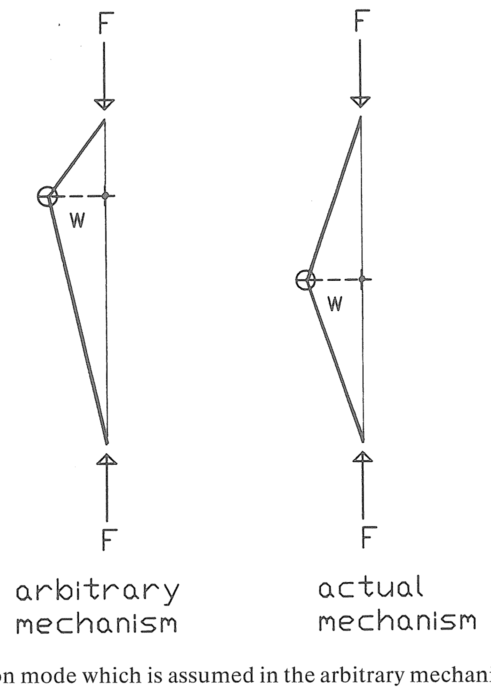

Fig. 3. The deformation mode which is assumed in the arbitrary mechanism is never attained in the actual mechanism.

the load-deformation behavior of the structure. This fact is often disregarded in the literature.

4.2 *Yield condition*

In general for steel the Von Mises yield surface is a valid yield condition. In generalized yield line theory stress resultants or generalized stresses rather than components of the stress tensor are used. Therefore a yield surface which is expressed in these generalized stresses is needed. As in limit analysis, there are two approaches used in determining a yield surface expressed in terms of generalized stresses, namely a static approach and a kinematic approach (Save and Massonnet, [22]). In the static approach, which is probably best known, a stress distribution which satisfies the yield condition is assumed over the cross section of the plate. These stresses are integrated over the thickness of the plate to produce the yield surface in terms of generalized stresses. In the kinematic approach a strain rate distribution is assumed over the cross section of the plate, the corresponding stress distribution is calculated by applying the normality rule to the yield condition and the yield surface in terms of generalized stresses is once more found by integrating these stresses over the thickness of the plate.
Out [15, 16] pointed out that upper bound limit analysis requires the yield surface to be derived on a kinematic basis. A kinematically induced yield surface will be an upper bound to the real yield surface whereas a statically induced yield surface may lie inside the real yield surface.
Out[1] also derived a kinematically induced yield surface for use in generalized yield line theory, accounting for bending moments, normal forces and in-plane shear forces (see Appendix A). This yield surface is an upper yield surface of the Von Mises yield surface. Because the Von Mises yield surface is strictly convex the upper yield surface does not coincide with it, and therefore the complete solution in generalized yield line theory cannot be found by refining the yield line pattern (see section 3.2.).
Out furthermore compared the kinematically induced yield surface with three different statically induced yield surfaces and noted that the statically induced surfaces are closer to the kinematically induced surface when the stress distributions show better resemblance.

4.3 *Fully plastic moment, normal force and shear force*

In generalized yield line theory it is often assumed that the fully plastic normal force n_p and the fully plastic moment m_p per unit length of a steel plate are equal to:

$$m_p = 1/4 \cdot t_p^2 \cdot f_y, \qquad (4.1)$$

$$n_p = t_p \cdot f_y \qquad (4.2)$$

[1] The same yield surface was derived by Dean [4], but the derivation by Out is more general.

These expressions are derived for fully plastic beams. They are not valid for plates because in a plate yield line the strain rate tensor component $\dot{\varepsilon}_{ss}$ vanishes since the length of the yield line does not change. The correct expressions for the fully plastic moment, normal force and shear force will now be derived.
Expressing the stresses in the x_n-x_s-x_z coordinate system (see Fig. 4) and taking account of the symmetry of the stress tensor, the Von Mises yield criterion can be written as:

$$\psi = \sigma_{nn}^2 + \sigma_{ss}^2 + \sigma_{zz}^2 - \sigma_{nn} \cdot \sigma_{ss} - \sigma_{ss} \cdot \sigma_{zz} - \sigma_{zz} \cdot \sigma_{nn} + 3 \cdot (\sigma_{ns}^2 + \sigma_{sz}^2 + \sigma_{zn}^2) - f_y^2 = 0. \quad (4.3)$$

It is assumed that the strain rate components $\dot{\varepsilon}_{nz}$ and $\dot{\varepsilon}_{sz}$ are equal to zero, because shear deformation is limited to the s-n plane (see also Appendix B, section B.1). From the normality condition it can be concluded that

$$\sigma_{nz} = \sigma_{sz} = 0, \quad (4.4)$$

and since the plate is assumed to be thin

$$\sigma_{zz} = 0. \quad (4.5)$$

Taking $\dot{\varepsilon}_{ss} = 0$ and applying the normality condition results in:

$$\dot{\varepsilon}_{ss} = \lambda \cdot \frac{\partial \psi}{\partial \sigma_{ss}} = \lambda \cdot (2 \cdot \sigma_{ss} - \sigma_{nn}) = 0, \quad (4.6)$$

where λ is a positive constant of proportionality. From equation (4.6) it can be seen that

$$\sigma_{ss} = \sigma_{nn}/2. \quad (4.7)$$

The Von Mises yield surface then reduces to:

$$\psi = 3/4 \cdot \sigma_{nn}^2 + 3 \cdot \sigma_{ns}^2 - f_y^2 = 0. \quad (4.8)$$

If $\sigma_{ns} = 0$ yielding will occur if

$$\sigma_{nn} = 2/\sqrt{3} \cdot f_y, \quad (4.9)$$

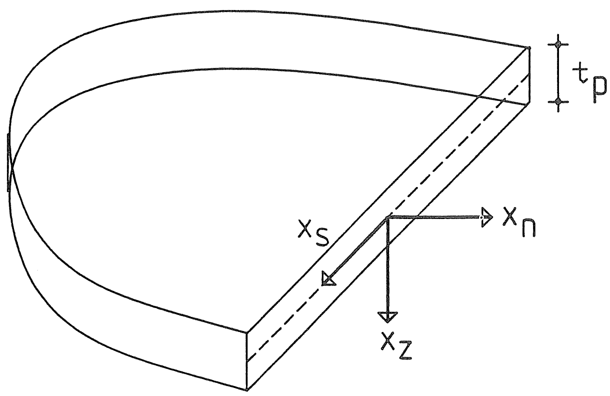

Fig. 4. Orientation of local coordinate axis in a yield line.

and if $\sigma_{nn} = 0$ yielding will occur if

$$\sigma_{ns} = 1/\sqrt{3} \cdot f_y. \tag{4.10}$$

Therefore, the correct expressions for the fully plastic moment, normal force and shear force per unit length are:

$$m_p = 1/4 \cdot t_p^2 \cdot 2/\sqrt{3} \cdot f_y, \tag{4.11}$$

$$n_p = t_p \cdot 2/\sqrt{3} \cdot f_y, \tag{4.12}$$

$$s_p = t_p/\sqrt{3} \cdot f_y. \tag{4.13}$$

These correct expressions were used by Dean [4] and Out [16], but in most other yield line applications (Narayanan and Chow [14], Packer and Davies [17], and Murray [11, 12]) the expressions 4.1 and 4.2 were used.

4.4 *Validity of generalized yield line theory*

Generalized yield line theory is based on a "small displacement (gradient)" Lagrangian formulation (see Appendix B, section B.3). This imposes restrictions on the validity of generalized yield line theory. These restrictions are explained in Appendix B and will be summarized here. They were not described explicitly in literature before.
Yield lines are simplifications of yield zones as they occur in reality. For a yield zone in which a bending moment, a normal force and an in-plane shear force are active, generalized yield line theory is valid only if:

$$\Delta\varphi \ll 1 \text{ [rad]}, \tag{4.14}$$

$$\Delta u_n \ll \delta, \tag{4.15}$$

$$\Delta u_s \ll \delta, \tag{4.16}$$

where $\Delta\varphi$ is the rotational deformation in the yield zone, Δu_n the normal deformation, Δu_s the in-plane shear deformation and δ the width of the yield zone. For yield zones with only a bending moment or only a shear force these limitations do not apply. For a yield line with only a normal force the theory is valid only if $\Delta u_n \ll \delta$.
In generalized yield line theory the width δ of the yield zone is a fictitious quantity. Its magnitude is undetermined. One might conclude therefore that the restrictions (4.15) and (4.16) have no practical importance because the limitations on the normal deformation Δu_n and the in-plane shear deformation Δu_s can be eliminated by assuming a large width of the yield zone. It must be noted however that in the derivation of the kinematic equations of a yield line mechanism (see section 5.3) the assumption is made that the width of the yield zones is so small (compared to the width of the rigid plate elements) that the yield zones may be considered as yield lines.

5 Work methods

In the work method a strictly kinematic approach is used and thus the method is fully consistent with upper bound limit analysis. The method was developed by Dean [4]. Out [15, 16] applied the method to calculate the post-buckling behavior of an in-plane loaded square plate and commented on some of its aspects. Because the work method is rather complex some simple problems are solved in Appendix C, so that the reader may get a better understanding of the method.

The work method can be summarized as follows:

1. Assume a yield line mechanism, that is choose a yield line pattern and determine the velocities of the rigid plane elements.
2. Determine the yield line deformation rates from the rigid plane element velocities by using the kinematic equations. These equations are discussed in section 5.3.
3. Determine the yield line forces by applying the normality rule to the (kinematically induced) yield surface and inserting the yield condition.
4. Calculate an upper bound for the limit load of the structure at any deformation state by equating the rate of energy dissipated in plastic flow in the yield lines to the rate of work performed by the external loads.

Some remarks have to be made about the determination of a yield line mechanism in generalized yield line theory. In generalized yield line theory, as in classical yield line theory, the structure to be analyzed is thought to consist of rigid plane elements joined by yield lines in which all deformation is postulated to occur. But where as in classical yield line only bending moments[2] are active in the yield lines, in generalized yield line theory normal and in-plane shear forces can also occur. The normality condition requires that in a yield line where a bending moment and normal and shear forces are active, rotational and normal and in-plane shear deformations must occur. The normal and in-plane shear deformations in the yield lines are determined by the movements of the rigid plane elements relative to each other. This means that a mechanism is no longer determined by the choice of a yield line pattern alone, as is the case in classical yield line theory, but by both the choice of a yield line pattern and the determination of the velocities of the rigid plane elements. It is possible to define different mechanisms for the same yield line pattern. The different kind of mechanisms that can be distinguished for the same yield line pattern will be discussed in the next section.

5.1 *Equilibrium and non-equilibrium mechanisms*

It can be deduced from the theorems of limit analysis that a necessary but not sufficient condition for finding the complete solution is the satisfaction of the in-plane equili-

[2] In classical yield line theory not only bending moments, but also torsional moments and transverse shear forces are active in the yield lines. This becomes evident in the equilibrium approach where the effect of torsional moments and transverse shear forces is accounted for by the concept of nodal forces. However, the bending moments are the only yield line forces that contribute to the energy dissipation.

brium of the plane elements. It is possible to determine the velocities of the rigid plane elements in such a way that this condition is satisfied (Dean [4] and Out [16]). A mechanism satisfying the in-plane equilibrium of the rigid plane elements will be called an equilibrium mechanism, whereas any mechanism not satisfying this condition will be called a non-equilibrium mechanism.

The equilibrium mechanism will probably result in the lowest limit load for the yield line pattern under consideration, but not necessarily in the exact limit load. Local equilibrium may still be violated as may the yield condition. Conditions on the intersection of yield lines, necessary for obtaining the complete solution, as discussed in section 3.2 have not yet been derived for generalized yield line theory. Also, since the kinematically derived upper yield surface does not coincide with the Von Mises yield surface, the exact limit load cannot be obtained by refining the yield line pattern. Only the exact limit load corresponding to the upper yield surface can be found. But even finding the exact limit load corresponding to the upper yield surface may be too difficult in practice, because the analysis becomes increasingly complex with an increasing number of yield lines and rigid plane elements.

As discussed in section 4.1 (generalized) yield line theory will result in the exact load-deformation curve of the structure only if the complete solution at every deformation stage is known. If this is not the case the analysis will not result even in an upper bound of the load-deformation behavior of the structure. Since neither an equilibrium mechanism nor a non-equilibrium mechanism will result in a complete solution there is no reason why an equilibrium mechanism would result in a better estimate of the load-deformation behavior of the structure than a non-equilibrium mechanism. This is illustrated by the analysis of an in-plane loaded square plate as shown in Fig. 5. For the assumed diagonal yield line pattern, two different mechanism were determined, an equilibrium mechanism and a non-equilibrium mechanism. The non-equilibrium mechanism is defined by assuming that the vertices of plane elements 1 and 3 remain connected during increasing lateral deflections. The solution for the equilibrium mechanism was given by Out [16] while the solution for the non-equilibrium mechanism was determined by the author. The results of the analysis of the two mechanisms are shown in Fig. 6 together with the results of a finite element analysis. It should be remembered that the yield line analysis results in a plastic unloading curve which is supposed to coincide with the actual load-deformation curve of the structure (in this case simulated with a finite element calculation) only after failure of the structure. As expected for the undeformed plate the equilibrium mechanism results in the lowest limit load. But for increasing deformations the non-equilibrium mechanism results in lower limit loads. In this case the non-equilibrium mechanism results even in a better prediction of the load-deformation behavior of the plate than the equilibrium mechanism. This is luck, the non-equilibrium mechanism might as well have resulted in a worse prediction. The equilibrium and non-equilibrium mechanisms are seen in Fig. 7 to be different. The in-plane deformations for both mechanisms are shown in this figure as a function of the lateral deflection of the plate.

In general a mechanism is determined if all the instantaneous positions and velocities

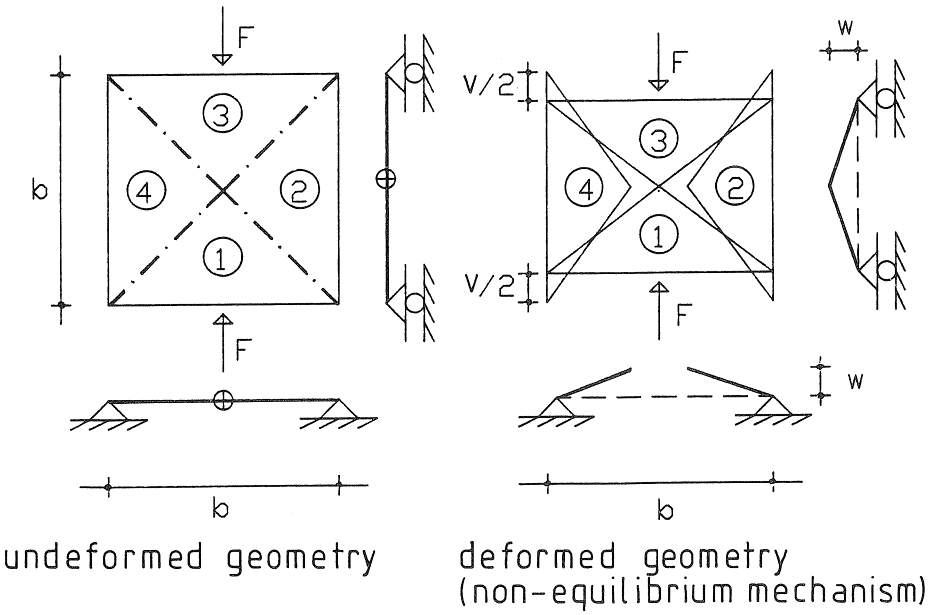

Fig. 5. Geometry of analyzed in-plane loaded square plate.

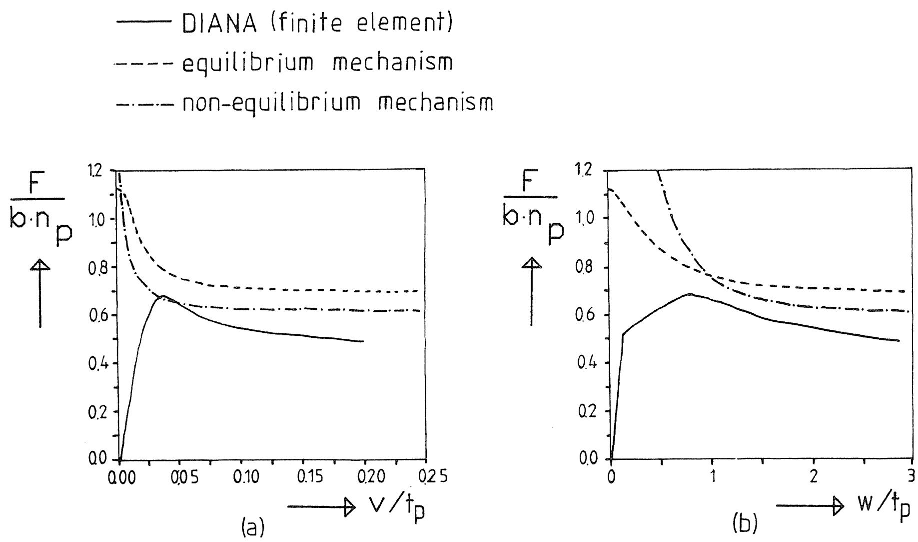

Fig. 6. Results of the analysis of in-plane loaded square plate.
a. Load as a function of the in-plane deformation *v*.
b. Load as a function of the lateral deflection *w*.

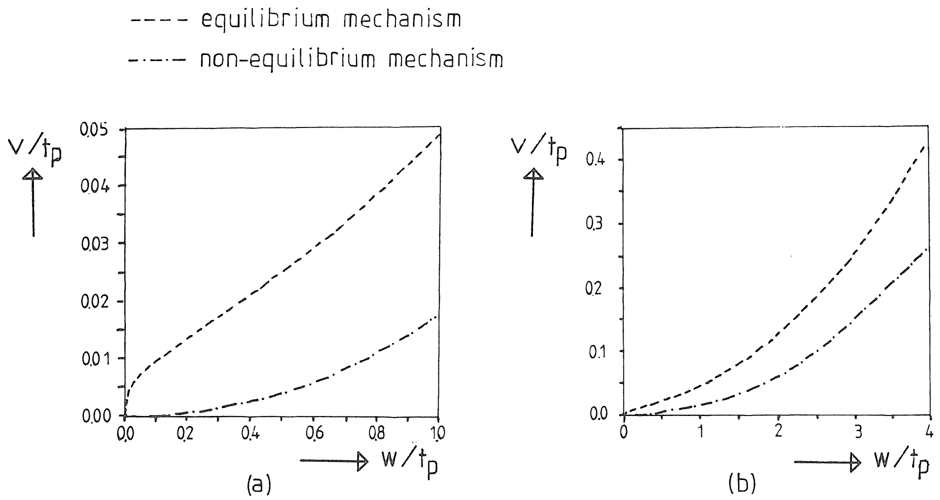

Fig. 7. Relation between lateral deflection and in-plane deformations for the equilibrium and the non-equilibrium mechanism for
a. small lateral deflections
b. large lateral deflections.

of the rigid plane elements are known as a function of only one deformation and one deformation rate parameter. In an equilibrium mechanism one starts to determine the positions and velocities of the rigid plane elements as a function of two or more deformation rate parameters. Requiring that the in-plane equilibrium of the plane elements is satisfied results in a set of equations from which the redundant deformation rates can be determined as a function of only one deformation rate parameter, and hence in the determination of the mechanism (Dean [4] and Out [16]). In many cases it is very difficult to determine an equilibrium mechanism, but fortunately it is often relatively easy to define a non-equilibrium mechanism. In a non-equilibrium mechanism the positions and velocities of the rigid plane elements are determined directly as a function of only one deformation rate parameter. Since the velocities of a rigid plane element are determined by the velocities of the vertices of the plane element we can define a non-equilibrium mechanism by assuming that certain vertices remain linked during deformation. In other words: normal and in-plane shear deformations are precluded in these points. The choice of these vertices is arbitrary but should be made in such a way that a mechanism is possible. If these non-equilibrium mechanisms are chosen in a reasonable way (that is the occurrence of membrane stresses in the mechanism should correspond to actual stresses in the structure) then it can be expected that they will give useful results. In Appendix D an example of the determination of the non-equilibrium mechanism is given for the in-plane loaded square plate described earlier in this section.

5.2 *True and quasi mechanisms*

Murray [11, 12] distinguished two major classes of plastic mechanisms, the so-called true mechanisms and the so-called quasi mechanisms. A true mechanism is a mechanism which can develop with only rotational deformations in the yield lines whereas a quasi mechanism is a mechanism which can develop only if also normal or in-plane yield line deformations occur in (some of) the yield lines. If one tries to make a cardboard model of a quasi mechanism, one will have to make some cuts in the cardboard to enable the model to deform.

For a true mechanism a non-equilibrium mechanism solution can be defined with only bending moments active in the yield lines. Normal and in-plane shear force, and hence in-plane displacements of the rigid plane elements relative to each other, need to be considered only if one wants to satisfy the in-plane equilibrium of the rigid plane elements. Since in a true mechanism the normal and in-plane shear forces can be determined from equilibrium considerations alone, the same result can be obtained by reducing the plastic moment in the yield lines for the presence of normal and shear forces (see also chapter 6). This is often easier to do since then the influence of the in-plane velocities of the rigid plane elements on the kinematic equations needs not be considered.

5.3 *Kinematic equations*

The generalized strain rates or yield line deformation rates used in generalized yield line theory are the rotational deformation rate $\Delta\dot{\varphi}$, the normal deformation rate $\Delta\dot{u}_n$ and the shear deformation rate $\Delta\dot{u}_s$ (see Appendix B, section B.1). In this section it will be explained how the yield line deformations and deformation rates can be determined from the velocities and instantaneous positions of the (vertices of the) rigid plane elements. The exact algorithms are not given, all calculations can be made with simple vector calculus. Yield lines are simplifications of yield zones as they occur in reality (see Appendix B, section B.3). The derivation of the kinematic equations below is based on the assumption that the width of the yield zones is so small (compared to the width of the rigid plane elements) that the yield zones may be considered as yield lines.

In Fig. 8 two adjacent plane elements linked by a yield line are shown. In the deformation state of the structure the yield line is determined as the line of intersection of the two planes containing the plane elements. The length of the yield line equals the length of the sides of the plane elements coinciding in the undeformed state. The rotational deformation $\Delta\varphi$ in the yield line equals the difference between the actual and the initial angle between the plane elements. Since the length of the yield line does not change during deformation, every point P_0 on the yield line can be associated with two points P_1 and P_2 on the plane elements 1 and 2 with which it initially coincided. The axial deformation Δu_n and the shear deformation Δu_s can then be calculated from the vectors $\underline{a}_1$ and $\underline{a}_2$, from P_0 to P_1 respectively P_0 to P_2(see Fig. 8). Each vector $\underline{a}_i$ can be resolved into a component $\underline{a}_{si}$ in the direction of the yield line and a component $\underline{a}_{ni}$ normal to the yield line. Then, Δu_n can be calculated as

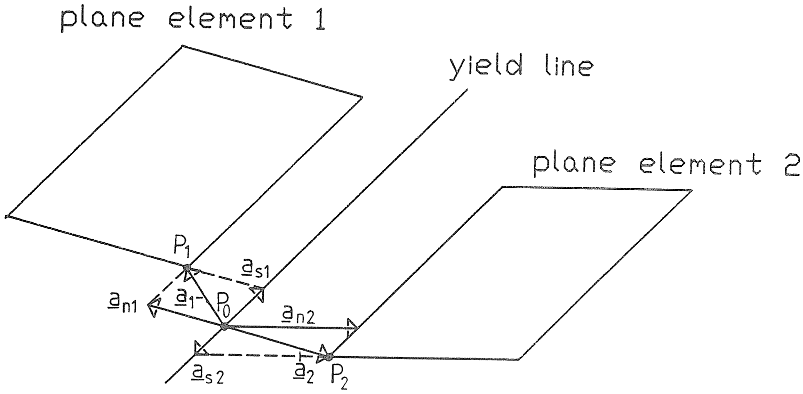

Fig. 8. Mechanism geometry for derivation of kinematic equations.

$$\Delta u_n = |\underline{a}_{n1} - \underline{a}_{n2}|, \tag{5.1}$$

and Δu_s can be calculated as

$$\Delta u_s = |\underline{a}_{s1} - \underline{a}_{s2}|. \tag{5.2}$$

The angle of rotation $\Delta\varphi$ is constant over the length of the yield line. The normal deformation Δu_n and shear deformation Δu_s may vary linearly. Therefore the deformations at any point of the yield line can be calculated from the deformations at two different points of the yield line. For these points the end points of the yield line are chosen. The yield line deformation rates can be determined from the yield line deformations by the equations:

$$\Delta \dot{u}_n = \frac{d\Delta u_n}{dt}, \tag{5.3}$$

$$\Delta \dot{u}_s = \frac{d\Delta u_s}{dt}, \tag{5.4}$$

and

$$\Delta\dot{\varphi} = \frac{d\Delta\varphi}{dt}. \tag{5.5}$$

In the kinematic equations used by Dean [4] and Out [16] second order polynomial approximations were used, that is $\sin\varphi$ was approximated by φ and $\cos\varphi$ was approximated by $(1 - 1/2 \cdot \varphi^2)$. It is not necessary to use these approximations.

6 Equilibrium method

In the equilibrium method the yield line mechanism is thought to consist of independent strips parallel to the direction of loading (see Fig. 9). The load carrying capacity of

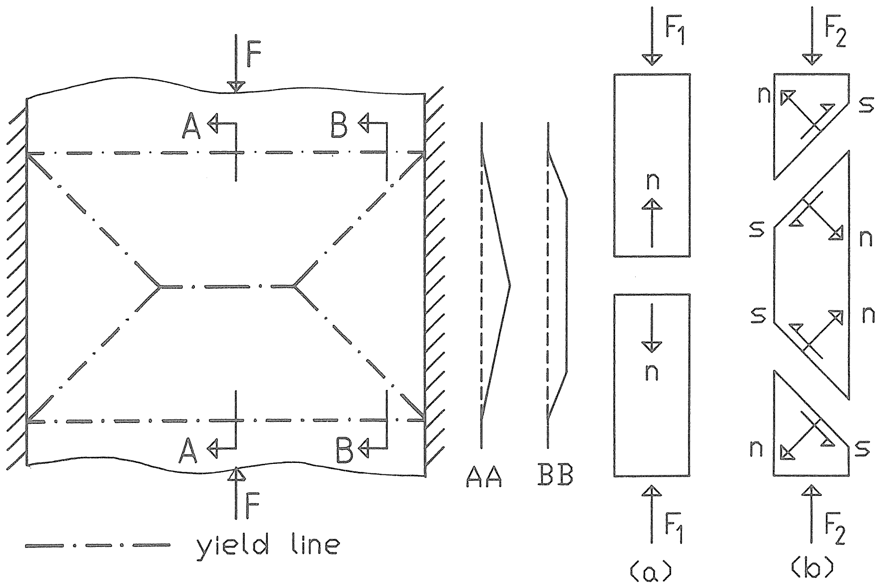

Fig. 9. An example of a plastic mechanism, shown with two characteristic strips:
a. mid-zone unit strip
b. edge zone unit strip.

each strip at any deformed geometry is calculated by safisfying the equilibrium of the strip under the condition that the forces in the yield line (moment, normal force and shear force) satisfy the yield condition. The capacity of the whole plate is found by integrating the limit loads of all the strips.

The strip equilibrium method differs from the equilibrium method in classical yield line analysis, where the equilibrium of the whole rigid segment is considered. In classical yield line theory it was proven that the equilibrium method is equivalent to the work method. However, it is quite easy to show that this is not the case in generalized yield line theory.

1. With the strip method only equilibrium mechanisms can be found while with the work method also non-equilibrium mechanisms can be defined.
2. In the strip method the normality condition is not satisfied. For a true mechanism the work method and the equilibrium method may give the same results. This is caused by the fact that in a true mechanism the forces in the yield line can be determined from equilibrium considerations alone. For a quasi mechanism however the normality rule is needed to derive the forces in the yield line and therefore the strip method cannot be used for the analysis of quasi mechanisms. It must be noted that Murray and Khoo [11] used the strip method to analyze “structural mechanisms” which are quasi mechanisms, but in their analysis they assumed that the fully plastic zones which appear in quasi mechanisms are either tension yield zones, compression yield zones or shear yield zones, without any interaction of a bending moment.

3. The kinematically derived yield surface can only be given in a parametric representation, i.e. as a function of the deformation rate parameters in the yield lines. This makes this yield surface unsuitable for use in the strip method. In the strip method therefore statically induced yield surfaces are used, which are not consistent with upper bound limit analysis.

The equilibrium approach was used by Davies, Kemp and Walker [3], by Murray [11, 12, 13] and by Narayanan and Chow [14][3]. These applications differ in the yield surface used. In the strip method developed by Murray the yield surface that was used is not explicitly mentioned. Since Murray has published quite extensively on yield line mechanisms in thin walled steel structures in may be interesting to investigate the yield surface he used in more detail.

6.1 *Murray's yield surface*

Murray's strip method is based on the use of an expression for the moment-capacity of a plastic hinge inclined at an angle β to that direction (see Fig. 10). It can be shown however that this expression is not based on a yield surface and therefore theoretically incorrect.

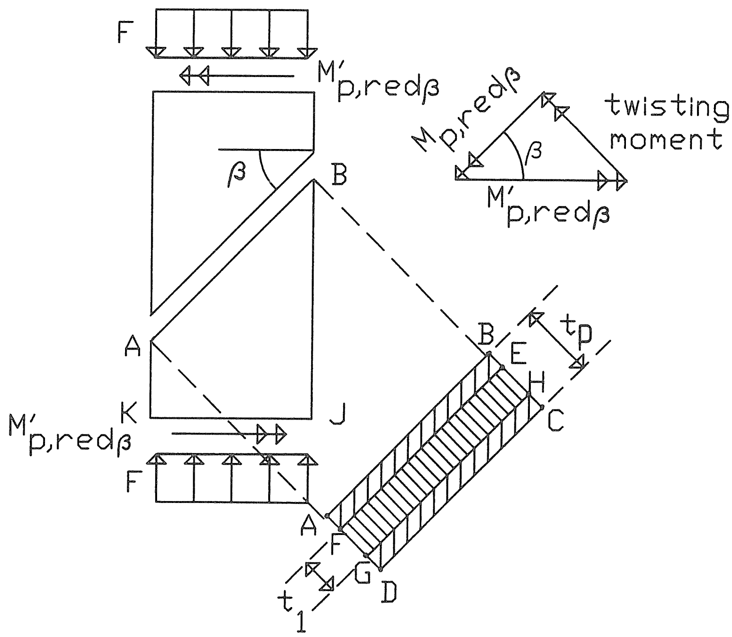

Fig. 10. Derivation of the moment capacity of a yield line inclined at an angle β to the direction of thrust.

[3] Davies, Kemp and Walker [3] actually referred to their method as the strip approach. Narayanan and Chow [14] and Murray [12, 13] did not explicitly define their methods as equilibrium or strip methods.

First the derivation by Murray is given. The moment capacity $M_{p,red}$ of a plastic hinge in a rectangular strut is given by the equation:

$$M_{p,red} = M_p \cdot (1 - F^2/F_p^2) = M_p \cdot (1 - t_1^2/t_p^2), \tag{6.1}$$

where $M_p = 1/4 \cdot t_p^2 \cdot f_y \cdot b$ is the plastic moment of the strip, $F_p = t_p \cdot f_y \cdot b$ is the yield force of the plate and t_1 is the thickness of the central core of the plate carrying the axial load F:

$$t_1 = F/(f_y \cdot b). \tag{6.2}$$

When the yield line is inclined at an angle β to the direction of thrust it is again assumed that a central core of depth t_1 carries the axial load F and hence we still have:

$$t_1 = F/(f_y \cdot b). \tag{6.3}$$

The bending moment $M_{p,red\beta}$ carried by the remaining areas of the cross section is given by equation:

$$M_{p,red\beta} = 1/4 \cdot t_p^2 \cdot f_y \cdot b/\cos\beta \cdot (1 - t_1^2/t_p^2) = M_{p,red}/\cos\beta. \tag{6.4}$$

From rotational equilibrium of the element ABJK it can then be concluded that:

$$M'_{p,red\beta} = M_{p,red\beta}/\cos\beta = M_{p,red}/\cos^2\beta. \tag{6.5}$$

The error in this derivation is the assumption that the axial load F in an inclined yield line is carried by a core of the same thickness as in an yield line perpendicular to the direction of thrust. The load F can be decomposed in a component N normal to the yield line and a component S tangent to the yield line

$$N = F \cdot \cos B, \tag{6.6}$$

$$S = F \cdot \sin\beta. \tag{6.7}$$

Taking a yield condition (for instance the Von Mises yield condition, see section 4.3), the core areas needed to carry the normal force and the shear force in the field line can be calculated:

$$\tau = S/(t_S \cdot b/\cos\beta) = f_y/\sqrt{3} \rightarrow t_S = F \cdot \sqrt{3} \cdot \sin\beta \cdot \cos\beta/(b \cdot f_y) \tag{6.8}$$

$$\sigma = N/(t_N \cdot b/\cos\beta) = 2 \cdot f_y/\sqrt{3} \rightarrow t_N = F \cdot \sqrt{3} \cdot \cos\beta \cdot \cos\beta/(2 \cdot b \cdot f_y) \tag{6.9}$$

Hence it can be concluded that the total core area t_1 needed to carry the load P equals:

$$t_1 = t_S + t_N = F/(b \cdot f_y) \cdot (\sqrt{3} \cdot \sin\beta \cdot \cos\beta + 1/2 \cdot \sqrt{3} \cdot \cos^2\beta. \tag{6.10}$$

So it can be seen that the thickness of the core needed to carry the load F depends on the angle of inclination of the yield line.

7 Intuitive methods

In the intuitive methods mechanism approaches are used without following a flow rule. Basically it is assumed that only bending moments are active in the yield lines. The influence of normal or shear forces is sometimes accounted for by satisfying the yield condition in the yield lines, resulting in a reduction of the fully plastic moment in the yield line, but the magnitude of the normal and shear forces is determined from rather intuitive equilibrium considerations. The intuitive methods vary in the yield surface used (often the influence of in-plane shear forces is neglected) and in the accuracy of the calculation of the rotations in the yield lines.

The intuitive methods are theoretically not correct, but they are much simpler than the work method or the equilibrium method, and in some cases they have given good results. An example of an intuitive approach with good results is the mechanism solution to predict the web crippling failure load of plate girders subjected to patch loading by Roberts [21]. Another example is the analysis of the strength of overlapped joints in rectangular hollow section trusses by Packer and Davies [17].

8 Miscellaneous

8.1 *Moving yield lines*

In classical yield line theory a yield line is a line across which the rate of slope $\partial \dot{u}_z / \partial x_n$ is discontinuous, where $\dot{u}_z$ is the deflection rate of the middle surface and x_n is the direction in the plate normal to the yield line. So far only stationary yield lines were considered. However, Prager [19] showed that travelling or moving yield lines are also possible. This derivation is presented here in a simplified form and the equation for the rate of energy dissipation in a moving yield line is derived.

Let D denote a yield line (or in general: a line of discontinuity) which is either stationary or moves in the x_n-direction. The fact that a function f is continuous, but not continuously differentiable across D is expressed by the equation:

$$V \cdot \Delta \frac{\partial f}{\partial x_n} + \Delta \frac{\partial f}{\partial t} = 0. \tag{8.1}$$

In this equation V is the yield line velocity (the velocity of propagation of D), and Δ denotes discontinuities across D, for instance $\Delta\varphi = \varphi_+ - \varphi_- \cdot \Delta\varphi = 0$ means that φ is continuous across D. Equation 8.1 is called the kinematic condition at the line of discontinuity D.

Now let us consider a yield line in which only bending moments are active. Since the deflection u_z and the deflection rate

$$\dot{u}_z = \frac{\partial u_z}{\partial t}$$

are continuous across D the kinematic condition results in:

$$V \cdot \Delta \frac{\partial u_z}{\partial x_n} + \Delta \frac{\partial u_z}{\partial t} = 0 \rightarrow V \cdot \Delta \frac{\partial u_z}{\partial x_n} = 0, \tag{8.2}$$

and

$$V \cdot \Delta \frac{\partial \dot{u}_z}{\partial x_n} + \Delta \frac{\partial \dot{u}_z}{\partial t} = 0. \tag{8.3}$$

For a stationary yield line $V = 0$ and it can be concluded that the slope $\partial u_z / \partial x_n$ may be discontinuous across D (and therefore the rate of slope $\partial \dot{u}_z / \partial x_n$) while the acceleration $\partial \dot{u}_z / \partial t$ must be continuous.
Considering a moving yield line ($V \neq 0$) it can be concluded that the slope $\partial u_z / \partial x_n$ must be continuous. The kinematic condition for the slope $\partial u_z / \partial x_n$ then results in:

$$V \cdot \Delta \frac{\partial^2 u_z}{\partial x_n^2} + \Delta \frac{\partial \dot{u}_z}{\partial x_n} = 0 \rightarrow \Delta \varkappa = -\Delta \frac{\partial^2 u_z}{\partial x_n^2} = \Delta \frac{\partial \dot{u}_z}{\partial x_n} / V \tag{8.4}$$

Since the rate of slope $\partial \dot{u}_z / \partial x_n$ is not continuous across D it can be concluded that the curvature changes instantaneously when the yield line moves across a particle in the plate. Denoting the rate of slope $\partial \dot{u}_z / \partial x_n$ at the other side of the moving yield line by $\dot{\theta}$, and the curvature by $\varkappa$, it can be seen that an initially flat plate element is curved into a constant radius $\varkappa = 1/R$ (see Fig. 11) if the yield line velocity V is equal to:

$$V = \dot{\theta} \cdot R. \tag{8.5}$$

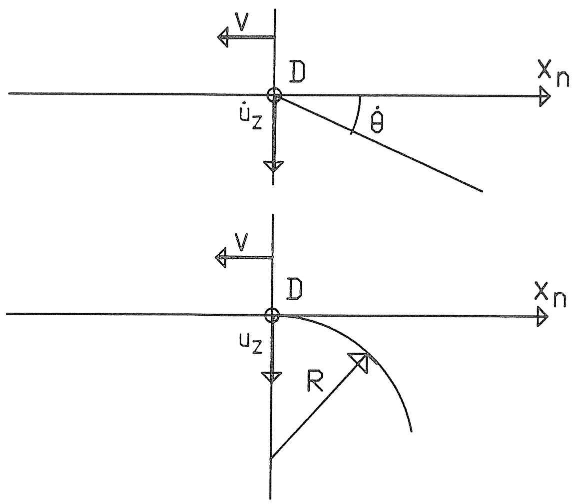

Fig. 11. Velocity and displacement fields at a moving yield line.

The rate of energy dissipation per unit width of the plate can then be calculated as:

$$\dot{W}_{int} = m_p \cdot \dot{\theta} = m_p \cdot V/R. \tag{8.6}$$

In a moving yield line the slope $\partial u_z / \partial x_n$ must be continuous. In the crushing process of thin-walled steel structures sometimes moving "fold lines" are observed (Abramowicz and Wierzbicki [1] and Wierzbicki and Abramowics [24]). A moving fold line can be modeled by the concept of two moving yield lines (see Fig. 12). The first moving

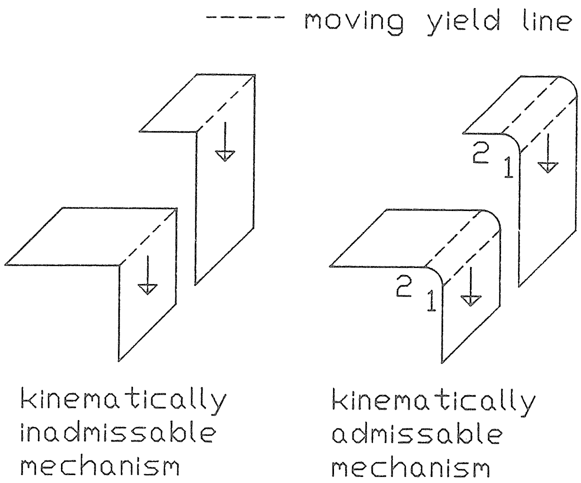

Fig. 12. Kinematically inadmissible and admissible folding mechanism.

yield line bends the plate into a curvature and the second yield line straightens the plate again. This process is referred to as a rolling process in literature.
An example of a (intuitive) mechanism solution including moving yield lines can be found in a paper by Kecman [9]. A theoretically more exact mechanism solution including moving yield lines was given by Wierzbicki and Abramowicz [24].

8.2 *Curved yield lines*

In yield line theory the structure to be analyzed is thought to consist of rigid plane elements joined by yield lines. Since the line of intersection of two planes is always a straight line only straight yield lines are possible. However, mechanisms with curved yield lines (see Fig. 13) were reported by Davies, Kemp and Walker [3], by Murray [11, 12, 13], and by Dean [4]. Both Dean and Murray proposed a solution for a mechanism with curved yield lines, Dean's solution was based on the work method, and Murray's was based on the equilibrium method. The solution is possible by assuming that while the rigid plane elements are rigid for in-plane deformations, they may be flexible for out-of-plane bending. It is interesting to note that Dean's circular yield arc mechanism is a quasi mechanism while Murray claimed that his flip-disc mechanism is a true mechanism (see Fig. 13). However, when one tries to fold the flip-disc mechanism from cardboard one discovers that actually it is a quasi mechanism too. But in order to be able to analyze this mechanism with the equilibrium method Murray had to assume it was a true mechanism.

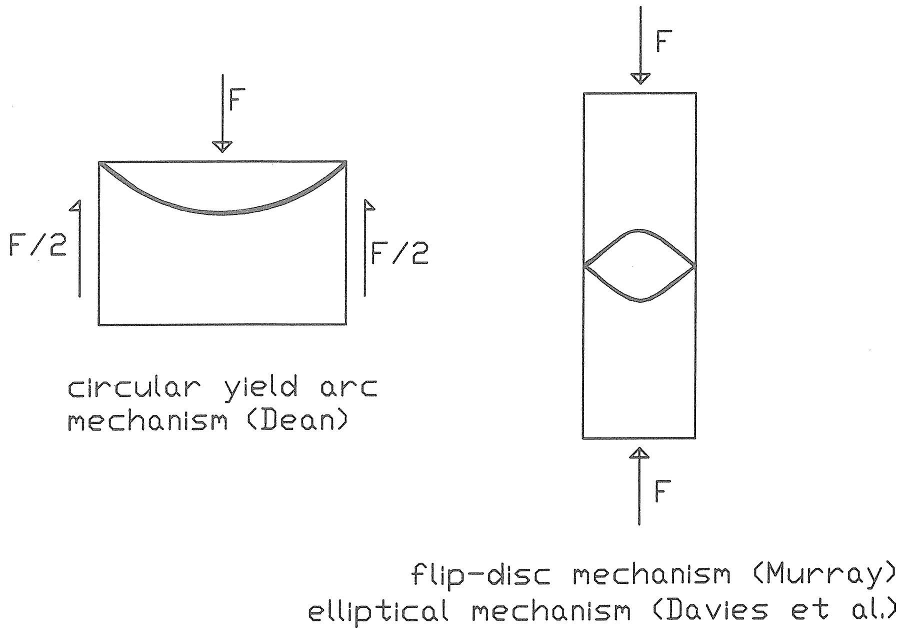

Fig. 13. Yield line mechanisms with curved yield lines.

8.3 *Determining a yield line pattern*

In all applications of yield line theory for the analysis of the load-deformation behavior of thin-walled steel members, the assumed yield line pattern was based primarily on observations in tests.
Davies, Kemp and Walker [3] determined one of the parameters of the yield line pattern by minimizing the failure load for the initial, undeformed structure, taking into account the effect of initial imperfections. If one tries to use the same approach to determine the yield line pattern in the deformed structure, it will often be found that for increasing deformations the optimal mechanism will change. Out [16] for instance noted: "for increasing deflection, different mechanisms, with a refined yield line pattern, produce lower approximations for the collapse behavior." It must be noted that if it is assumed that the yield line pattern changes during deformation, some yield lines must be moving yield lines instead of stationary yield lines. In some applications of yield line theory, for instance in the mechanism solution for patch loading on plate girders by Roberts [21], this aspect is neglected.
Murray [13] stated that the local plastic mechanisms which develop in thin-walled structures are a by-product of the elastic buckles formed during the rising part of the load path. He reported two types of mechanisms in box-columns with axial loading, namely the flip-disc mechanism and the roof mechanism (see Fig. 14). The flip-disc mechanism developed when first yield occurred at the edges of the plate while the

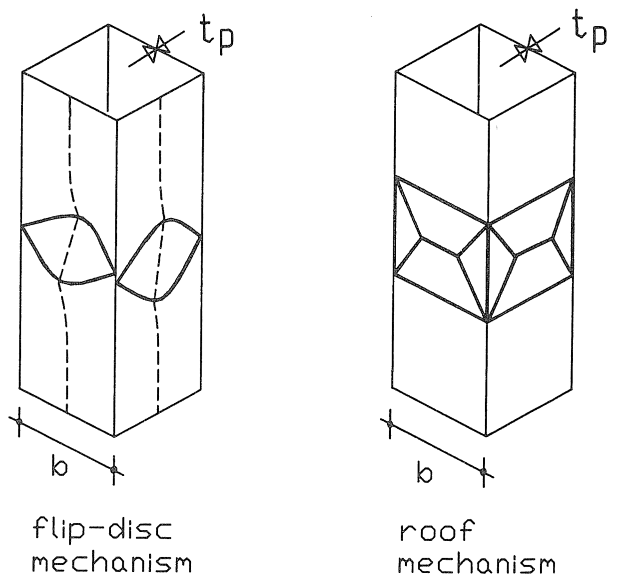

Fig. 14. The two plastic mechanisms observed in box-columns with axial load only.

roof mechanism developed when first yield occurred at the centre of the plate, the place of first yield being determined by the b/t_p ratio of the plate and the initial imperfections of the plate. So Murray concluded that "the location of a plastic mechanism is fixed by the point of first yield. It becomes attached to that point and cannot change either its position or form."

Murray's conclusions were restricted to the mechanisms observed in box-columns with axial load only. These mechanisms had stationary yield lines. It must be noted that a mechanism with moving yield lines can actually change its position and form.

9 Conclusions

1. Upper bound limit analysis results in a limit load for a structure at a certain deflected shape. It does not result in an upper bound for the load-deformation behavior of a structure (section 4.1).
2. Upper bound limit analysis requires the yield surface to be derived by the kinematic approach (section 4.2).
3. Yield line analysis can only lead to a complete solution if the upper yield surface corresponds to the actual yield surface (section 3.2). The kinematically induced yield surface derived by Dean [4] and Out [15, 16] for use in generalized yield line theory is an upper yield surface of the Von Mises yield surface, not coinciding with the Von Mises yield surface (section 4.2). Therefore, in generalized yield line theory, the exact limit load cannot be found by refining the yield line pattern.

4. For the Von Mises yield surface the expressions for the fully plastic moment, normal force and shear force in a yield line are (section 4.3):

$$m_p = 1/4 \cdot t_p^2 \cdot 2/\sqrt{3} \cdot f_y$$
$$n_p = t_p \cdot 2/\sqrt{3} \cdot f_y$$
$$s_p = t_p/\sqrt{3} \cdot f_y$$

5. For yield lines in which a bending moment, a normal force and an in-plane shear force is active, generalized yield line theory is only valid if $\Delta\varphi \ll 1$ [rad], $\Delta u_n \ll \delta$ and $\Delta u_s \ll \delta$, where $\Delta\varphi$ is the rotational deformation in the yield line, Δu_n the normal deformation, Δu_s the in-plane shear deformation and δ the width of the yield zone (section 4.4 and Appendix B, section B.3).
6. In generalized yield line theory a mechanism is determined by the choice of a yield line pattern and the determination of the velocities of the thus defined rigid plane elements (chapter 5).
   An equilibrium mechanism is a mechanism in which the velocities of the rigid plane elements are determined in such a way that the in-plane equilibrium of the rigid plane elements is satisfied. A non-equilibrium mechanism is any mechanism in which this equilibrium is not satisfied. In the analysis of the load-deformation behavior of a structure a non-equilibrium mechanism, which is much easier to analyze than an equilibrium mechanism, may give results as good as those obtained from an equilibrium mechanism (section 5.1).
7. A true mechanism is a mechanism which can develop with only rotational deformations in the yield lines. A quasi mechanism is a mechanism which can develop only with normal and/or shear deformations in (some of) the yield lines (section 5.2).
8. The work method is the only generalized yield line method being fully consistent with upper bound limit analysis (chapter 5).
   Equilibrium methods are not consistent with upper bound limit analysis because the flow rule is not satisfied (section 6.1).
   Both equilibrium and intuitive methods, although theoretically incorrect, have proven to be able to produce useful results.
9. Not only stationary yield lines, but also moving yield lines are possible. If an initially flat plate element is curved into a constant radius R by a moving yield line then the rate of energy dissipation per unit width in the yield line is given by:

$$\dot{W}_{int} = m_p \cdot V/R,$$

   where V is the velocity of the moving yield line (section 8.1).
10. Curved yield lines were observed in tests and can be modeled by assuming that the rigid plane elements are flexible in bending (section 8.2).
11. A yield line pattern has to be determined from observations in experiments. The actual yield line pattern is not necessarily the yield line pattern that minimizes the failure load. In axially loaded box columns the yield line pattern was proven to be determined by the place of first yield in the column (section 8.3).

10 Acknowledgements

This research was supported by the Netherlands Technology Foundation (STW). It was performed while the author worked as a research assistant at the Eindhoven University of Technology and at Cornell University (USA), and was first published as Report 89-7, Dept. of Civ. Eng., Cornell University. The author is indebted to prof. ir. A. C. W. M. Vrouwenvelder (Delft University of Technology) for his knowledge and discussions on the subject and reviewing this manuscript and its earlier versions. Also the guidance, advise and comments of prof. ir. J. W. B. Stark, ir. F. van Pelt (Eindhoven University of Technology) and prof. T. Peköz (Cornell University) are gratefully acknowledged.

11 Notations

a_i	displacement vector component $(i = n, s, z)$
$\dot{a}_i$	velocity vector component $(i = n, s, z)$
b	width of plate
F	force
f_y	uniaxial yield stress
n	normal force per unit length of yield line
n_p	fully plastic normal force per unit length of yield line
s	shear force per unit length of yield line
s_p	fully plastic shear force per unit length of yield line
t	time
t_p	thickness of plate
u_i	mid-plane displacement vector component $(i = n, s, z)$
$\dot{u}_i$	mid-plane velocity vector component $(i = n, s, z)$
v	in-plane displacement
V	volume, velocity
w	out of plane deflection
$\dot{W}$	rate of energy dissipation, rate of work
$\dot{W}_s$	rate of specific energy dissipation
x_n	in-plane coordinate axis normal to yield line
x_s	in-plane coordinate axis along yield line
x_z	coordinate axis perpendicular to plane of plate
δ	width of yield zone
Δu_n	normal deformation in yield line
$\Delta \dot{u}_n$	normal deformation rate in yield line
Δu_s	shear deformation in yield line
$\Delta \dot{u}_s$	shear deformation rate in yield line
$\Delta \varphi$	rotation in yield line
$\Delta \dot{\varphi}$	rotation deformation rate in yield line
$\dot{\varepsilon}_{ij}$	strain rate tensor components $(i, j = n, s, z)$
$\dot{\bar{\varepsilon}}$	normal strain rate at mid thickness

$\dot{\gamma}$ shear deformation rate
$\dot{\varkappa}$ rate of curvature
θ rotation of rigid plane element
$\dot{\theta}$ rotation rate of rigid plane element
ψ plastic potential function
σ_{ij} stress tensor components $(i,j = n, s, z)$

12 References

1. Abramowicz, W. and T. Wierzbicki, A kinematic approach to crushing of shell structures, In: Third International Conference of Vehicle Structural Mechanics, SAE, Warrendale 1979, pp. 211–223.
2. Braestrup, M. W., Yield line theory and limit analysis of plates and slabs, Magazine of Concrete Research, Vol. 22, No. 71, pp. 99–106 (1970).
3. Davies, P., K. O. Kemp and A. C. Walker, An analysis of the failure mechanism of an axially loaded simply supported steel plate, Proceedings of the Institution of Civil Engineers, Part 2, Vol. 59, No. 59, pp. 645–658 (1975).
4. Dean, J. A., The collapse behaviour of steel plating subject subject to complex loading, Ph.D. Thesis, Imperial College of Science and Technology, London, 1975.
5. Drucker, D. C. and R. I. Providence, The effect of shear on the plastic bending of beams, ASME, Journal of Applied Mechanics, Dec. 1956, pp. 509–514.
6. Hill, R., The mathematical theory of plasticity, Oxford University Press, London, 1956.
7. Jones, L. L. and R. H. Wood, Yield line analysis of slabs, Thames & Hudson and Chatto & Windus, London, 1967.
8. Kachanov, L. M., Foundations of the theory of plasticity, North-Holland Pubishing Company, Amsterdam, 1971.
9. Kecman, D., Bending collapse of rectangular and square section tubes, International Journal of Mechanical Sciences, Vol. 25, No. 9–10, pp. 623–636 (1983).
10. Mase, G. E., Schaum's outline of theory and problems of continuum mechanics, McGraw-Hill Book Company, New York, 1970.
11. Murray, N. W. and P. S. Khoo, Some basic plastic mechanisms in the local buckling of thin-walled steel structures, International Journal of Mechanical Sciences, Vol. 23, No. 12, pp. 703–713 (1981).
12. Murray, N. W., Introduction to the theory of thin walled steel structures, Clarendon Press, Oxford, 1984.
13. Murray, N. W., Some phenomena observed in thin-walled square box-sections under axial, bending and torsional loading, In: Steel structures. Advances, design and construction, Proceedings of the International Conference on Steel and Aluminium Structures, ed. by R. Narayanan, Elsevier Applied Science, London, 1987.
14. Narayanan, R. and F. Y. Chow, Strength of biaxially compressed perforated plates, In: Proceedings of the Seventh International Specialty Conference on Cold-Formed Steel Structures, ed. by W. W. Yu and J. H. Senne, University of Missouri-Rolla, 1984.
15. Out, J. M. M., Yield surface for yield line theory based on a kinematical approach, Report No. BI-82-28, TNO Institute of Building Materials and Building Structures, Rijswijk, The Netherlands, 1981.
16. Out, J. M. M., Yield surface for bending moment, shear force and normal force, Heron, Vol. 30, No. 4, pp. 30–58 (1985).
17. Packer, J. A. and G. Davies, Ultimate strength of overlapped joints in rectangular hollow section trusses, Proceedings of the Institution of Civil Engineers, Part 2, Vol. 73, June, pp. 329–350 (1982).
18. Prager, W. and P. G. Hodge, Theory of perfectly plastic solids, John Wiley & Sons, New York, 1951.

19. Prager, W., Discontinuous fields of plastic stress and flow, In: Proceedings of the second U.S. National Congress of Applied Mechanics, ASME, Michigan, 1954.
20. Puthli, R. S., Geometrical non-linearity in collapse analysis of thick shells, with application to tubular steel joints, Heron, Vol. 26, No. 2, (1981).
21. Roberts, T. M., Patch loading on plate girders, In: Plated structures, stability and strength, ed. by R. Narayanan, Applied Science Publishers, London, 1983.
22. Save, M. A. and C. E. Massonnet, Plastic analysis and design of plates, shells and discs, North Holland Publishing Company, Amsterdam, 1972.
23. Washizu, K., Variational methods in elasticity and plasticity, Pergamon Press, Oxford, 1982.
24. Wierzbicki, T. and W. Abramowicz, On the crushing mechanics of thin-walled structures, Journal of Applied Mechanics, Vol. 50, Dec. 1983, pp. 727-734.

Appendix A: A kinematically derived yield surface

The kinematically derived yield surface is described by the following formulas:

$$\frac{m}{m_p} = \frac{\Delta\dot{\varphi}}{|\Delta\dot{\varphi}|} \cdot 1/2 \cdot \left[a^+ \cdot b^- - a^- \cdot b^+ - \omega_s^2 \cdot \ln\left(\frac{a^+ + b^+}{a^- + b^-}\right)\right], \quad \text{if } \Delta\dot{\varphi} \neq 0$$

$$= 0, \quad \text{if } \Delta\dot{\varphi} = 0 \qquad \text{(A.1)}$$

$$\frac{n}{n_p} = \frac{\Delta\dot{\varphi}}{|\Delta\dot{\varphi}|} \cdot 1/2 \cdot [b^+ - b^-], \quad \text{if } \Delta\dot{\varphi} \neq 0$$

$$= \frac{\Delta\dot{u}_n}{|\Delta\dot{u}_n|} \cdot 1/\sqrt{1 + (\omega_s/\omega_n)^2}, \quad \text{if } \Delta\dot{\varphi} = 0 \qquad \text{(A.2)}$$

$$\frac{s}{s_p} = \frac{\Delta\dot{\varphi}}{|\Delta\dot{\varphi}|} \cdot 1/2 \cdot \omega_s \cdot \ln\left(\frac{a^+ + b^+}{a^- + b^-}\right), \quad \text{if } \Delta\dot{\varphi} \neq 0$$

$$= \frac{\Delta\dot{u}_s}{|\Delta\dot{u}_s|} \cdot 1/\sqrt{1 + (\omega_n/\omega_s)^2}, \quad \text{if } \Delta\dot{\varphi} = 0 \qquad \text{(A.3)}$$

in which

$$m_p = 2/\sqrt{3} \cdot f_y (t_p/2)^2 \qquad \text{(A.4)}$$

fully plastic moment per unit length of yield line

$$n_p = 2/\sqrt{3} \cdot f_y \cdot t_p \qquad \text{(A.5)}$$

fully plastic normal force per unit length of yield line

$$s_p = 1/\sqrt{3} \cdot f_y \cdot t_p \qquad \text{(A.6)}$$

fully plastic in-plane shear force per unit length of yield line

$$\omega_n = \frac{n_p}{2m_p} \cdot \frac{\Delta\dot{u}_n}{\Delta\dot{\varphi}} \qquad \omega_s = \frac{s_p}{2m_p} \cdot \frac{\Delta\dot{u}_s}{\Delta\dot{\varphi}} \qquad \text{(A.7)}$$

$$a^+ = \omega_n + 1 \qquad a^- = \omega_n - 1 \qquad \text{(A.8)}$$

$$b^+ = \sqrt{(a^+)^2 + \omega_s^2} \qquad b^- = \sqrt{(a^-)^2 + \omega_s^2} \qquad \text{(A.9)}$$

$\Delta\dot{u}_n$ = normal deformation rate in yield line
$\Delta\dot{u}_s$ = shear deformation rate in yield line
$\Delta\dot{\varphi}$ = rotational deformation rate in yield line
n = normal force per unit length in yield line
s = in-plane shear force per unit length in yield line
m = bending moment per unit length in yield line

Equations A.1, A.2 and A.3 can be regarded as a parametric representation of the yield surface in generalized stress space.
For $m = 0$ this yield surface is represented by the equation:

$$(n/n_p)^2 + (s/s_p)^2 - 1 = 0. \qquad \text{(A.10)}$$

For $s = 0$ this yield surface is represented by the equation:

$$\frac{\Delta\dot{\varphi}}{|\Delta\dot{\varphi}|} \cdot (m/m_p) + (n/n_p)^2 - 1 = 0. \qquad \text{(A.11)}$$

Appendix B: Basic assumptions and validity of generalized yield line theory

In this appendix the basic assumptions of generalized yield line theory will be explained. Therefore first the yield line deformation rates and yield line forces are derived. Then the validity of the derived formulas will be discussed. Unless otherwise stated a Lagrangian description is used.

B.1 *Yield line deformation rates*

For the choice of the generalized strain rates first the character of the strain rate tensor in a yield zone as outlined by Out [15, 16] will be discussed. The orientation of the local coordinate axes in the yield zone is shown in Fig. 4. Generally, a strain rate tensor consists of six independent components. The following strain rate tensor components are assumed to be zero:

1. $\dot{\varepsilon}_{nz} (= \dot{\varepsilon}_{zn})$ and $\dot{\varepsilon}_{sz} (= \dot{\varepsilon}_{zs})$, since shear deformation is limited to the n-s plane. This assumption is equivalent to stating that straight lines initially normal to the middle surface remain straight and normal to that surface subsequent to bending. It implies that twisting curvature across the yield line is precluded.
2. $\dot{\varepsilon}_{ss}$, since the length versus width ratio of a yield line is large and the adjacent plate elements are rigid; incompressibility then implies that

$$\dot{\varepsilon}_{zz} = -\dot{\varepsilon}_{nn}. \qquad \text{(B.1)}$$

In the yield zone thus the following strain rate distribution is assumed (see Fig. 15):

$$\dot{\varepsilon}_{nn}(x_z) = \dot{\bar{\varepsilon}} + \dot{\varkappa} \cdot x_z, \qquad \text{(B.2)}$$

$$\dot{\varepsilon}_{zz}(x_z) = -\dot{\bar{\varepsilon}} - \dot{\varkappa} \cdot x_z, \qquad \text{(B.3)}$$

$$\dot{\varepsilon}_{ns}(x_z) = \dot{\varepsilon}_{sn}(x_z) = \dot{\gamma}/2, \qquad \text{(B.4)}$$

$$\dot{\varepsilon}_{ss} = \dot{\varepsilon}_{nz} = \dot{\varepsilon}_{zn} = \dot{\varepsilon}_{zs} = \dot{\varepsilon}_{sz} = 0. \qquad \text{(B.5)}$$

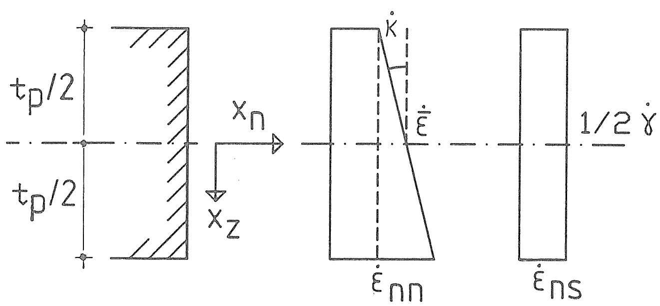

Fig. 15. Assumed strain rate distribution in a yield line.

The generalized strain rates are chosen to be:

$$\Delta\dot{u}_{\mathrm{n}} = \int_0^\delta \dot{\varepsilon} \cdot \mathrm{d}x_{\mathrm{n}} = \dot{\bar{\varepsilon}} \cdot \delta, \tag{B.6}$$

$$\Delta\dot{u}_{\mathrm{s}} = \int_0^\delta \dot{\gamma}/2 \cdot \mathrm{d}x_{\mathrm{n}} = \dot{\gamma}/2 \cdot \delta, \tag{B.7}$$

$$\Delta\dot{\varphi} = \int_0^\delta \dot{\varkappa} \cdot \mathrm{d}x_{\mathrm{n}} = \dot{\varkappa} \cdot \delta, \tag{B.8}$$

where δ is the width of the yield zone.

For a better understanding of the basic assumptions of the method the velocity field corresponding to the above described strain rate field will be discussed (Prager [18]). In a portion of a plate with thickness t_{p}, the axes x_{n} and x_{s} are chosen in the middle surface of the undeformed plate.

The following velocity field is considered:

$$\dot{a}_{\mathrm{n}} = \dot{u}_{\mathrm{n}} - x_{\mathrm{z}} \cdot \frac{\partial \dot{u}_{\mathrm{z}}}{\partial x_{\mathrm{n}}}, \tag{B.9}$$

$$\dot{a}_{\mathrm{s}} = \dot{u}_{\mathrm{s}} - x_{\mathrm{z}} \cdot \frac{\partial \dot{u}_{\mathrm{z}}}{\partial x_{\mathrm{s}}}, \tag{B.10}$$

$$\dot{a}_{\mathrm{z}} = \dot{u}_{\mathrm{z}} - x_{\mathrm{z}} \cdot \left(\frac{\partial \dot{u}_{\mathrm{n}}}{\partial x_{\mathrm{n}}} + \frac{\partial \dot{u}_{\mathrm{s}}}{\partial x_{\mathrm{s}}}\right) + 1/2 \cdot x_{\mathrm{z}}^2 \cdot \left(\frac{\partial^2 \dot{u}_{\mathrm{z}}}{\partial x_{\mathrm{n}}^2} + \frac{\partial^2 \dot{u}_{\mathrm{z}}}{\partial x_{\mathrm{s}}^2}\right), \tag{B.11}$$

where $\dot{u}_{\mathrm{z}}$, $\dot{u}_{\mathrm{n}}$ and $\dot{u}_{\mathrm{s}}$ are the rate of deflection and the in-plane displacement rates of the middle surface. The second and third term on the right-hand side of equation B.11 are necessary if the velocity field is to satisfy the condition of incompressibility:

$$(\dot{\varepsilon}_{\mathrm{nn}} + \dot{\varepsilon}_{\mathrm{ss}} + \dot{\varepsilon}_{\mathrm{zz}} = 0). \tag{B.12}$$

From this velocity field the following strain rate field can be calculated:

$$\dot{\varepsilon}_{\mathrm{nn}} = \frac{\partial \dot{a}_{\mathrm{n}}}{\partial x_{\mathrm{n}}} = \frac{\partial \dot{u}_{\mathrm{n}}}{\partial x_{\mathrm{n}}} - x_{\mathrm{z}} \cdot \frac{\partial^2 \dot{u}_{\mathrm{z}}}{\partial x_{\mathrm{n}}^2} \tag{B.13}$$

$$\dot{\varepsilon}_{\mathrm{ss}} = \frac{\partial \dot{a}_{\mathrm{s}}}{\partial x_{\mathrm{s}}} = \frac{\partial \dot{u}_{\mathrm{s}}}{\partial x_{\mathrm{s}}} - x_{\mathrm{z}} \cdot \frac{\partial^2 \dot{u}_{\mathrm{z}}}{\partial x_{\mathrm{s}}^2}, \tag{B.14}$$

$$\dot{\varepsilon}_{\mathrm{zz}} = \frac{\partial \dot{a}_{\mathrm{z}}}{\partial x_{\mathrm{z}}} = -\left(\frac{\partial \dot{u}_{\mathrm{n}}}{\partial x_{\mathrm{n}}} + \frac{\partial \dot{u}_{\mathrm{s}}}{\partial x_{\mathrm{s}}}\right) + x_{\mathrm{z}} \cdot \left(\frac{\partial^2 \dot{u}_{\mathrm{z}}}{\partial x_{\mathrm{n}}^2} + \frac{\partial^2 \dot{u}_{\mathrm{z}}}{\partial x_{\mathrm{s}}^2}\right), \tag{B.15}$$

$$\dot{\varepsilon}_{\mathrm{ns}} = \dot{\varepsilon}_{\mathrm{sn}} = 1/2 \cdot \left(\frac{\partial \dot{a}_{\mathrm{n}}}{\partial x_{\mathrm{s}}} + \frac{\partial \dot{a}_{\mathrm{s}}}{\partial x_{\mathrm{n}}}\right) = 1/2 \cdot \left(\frac{\partial \dot{u}_{\mathrm{n}}}{\partial x_{\mathrm{s}}} + \frac{\partial \dot{u}_{\mathrm{s}}}{\partial x_{\mathrm{n}}} - 2 \cdot x_{\mathrm{z}} \cdot \frac{\partial^2 \dot{u}_{\mathrm{z}}}{\partial x_{\mathrm{n}} \cdot \partial x_{\mathrm{s}}}\right), \tag{B.16}$$

$$\dot{\varepsilon}_{sz} = \dot{\varepsilon}_{zs} = 1/2 \cdot \left(\frac{\partial \dot{a}_s}{\partial x_z} + \frac{\partial \dot{a}_z}{\partial x_s}\right) =$$

$$1/2 \cdot \left(-x_z \cdot \left(\frac{\partial^2 \dot{u}_n}{\partial x_n \cdot \partial x_s} + \frac{\partial^2 \dot{u}_s}{\partial x_s^2}\right) + 1/2 \cdot x_z^2 \cdot \left(\frac{\partial^3 \dot{u}_z}{\partial x_n^2 \cdot \partial x_s} + \frac{\partial^3 \dot{u}_z}{\partial x_s^3}\right)\right), \qquad \text{(B.17)}$$

$$\dot{\varepsilon}_{xz} = \dot{\varepsilon}_{zx} = 1/2 \cdot \left(\frac{\partial \dot{a}_n}{\partial x_z} + \frac{\partial \dot{a}_z}{\partial x_n}\right) =$$

$$1/2 \cdot \left(-x_z \cdot \left(\frac{\partial^2 \dot{u}_n}{\partial x_n^2} + \frac{\partial^2 \dot{u}_s}{\partial x_n \cdot \partial x_s}\right) + 1/2 \cdot x_z^2 \cdot \left(\frac{\partial^3 \dot{u}_z}{\partial x_n^3} + \frac{\partial^3 \dot{u}_z}{\partial x_n \cdot \partial x_s^2}\right)\right). \qquad \text{(B.18)}$$

The following middle surface velocities are considered:

$$\dot{u}_n = \dot{u}_{no} + \frac{\Delta \dot{u}_n \cdot x_n}{\delta} \qquad \text{for } 0 \leq x_n \leq \delta$$

$$= \dot{u}_{no} + \Delta \dot{u}_n \qquad \text{for } x_n > \delta \qquad \text{(B.19)}$$

$$\dot{u}_s = \dot{u}_{so} + \frac{\Delta \dot{u}_s \cdot x_n}{\delta} \qquad \text{for } 0 \leq x_n \leq \delta$$

$$= \dot{u}_{so} + \Delta \dot{u}_s \qquad \text{for } x_n > \delta \qquad \text{(B.20)}$$

$$\dot{u}_z = \dot{u}_{zo} + \frac{\Delta \dot{\varphi} \cdot x_n^2}{2 \cdot \delta} \qquad \text{for } 0 \leq x_n \leq \delta$$

$$= \dot{u}_{zo} = \frac{\Delta \dot{\varphi}}{2} \cdot (2 \cdot x_n - \delta) \qquad \text{for } x_n > \delta \qquad \text{(B.21)}$$

Assuming constant velocities this results in the following (continuous but not continuously differentiable) displacement field:

$$u_n(t) = \dot{u}_n \cdot t = u_{no} + \frac{\Delta u_n \cdot x_n}{\delta} \qquad \text{for } 0 \leq x_n \leq \delta$$

$$= u_{no} + \Delta u_n \qquad \text{for } x_n > \delta \qquad \text{(B.22)}$$

where $u_{no} = \dot{u}_{no} \cdot t$ and $\Delta u_n = \Delta \dot{u}_n \cdot t$,

$$u_s(t) = \dot{u}_s \cdot t = u_{so} + \frac{\Delta u_s \cdot x_n}{\delta} \qquad \text{for } 0 \leq x_n \leq \delta$$

$$= u_{so} + \Delta u_s \qquad \text{for } x_n > \delta \qquad \text{(B.23)}$$

where $u_{so} = \dot{u}_{so} \cdot t$ and $\Delta u_s = \Delta \dot{u}_s \cdot t$,

$$u_z(t) = \dot{u}_z \cdot t = u_{zo} + \frac{\Delta \varphi \cdot x_n^2}{2 \cdot \delta} \qquad \text{for } 0 \leq x_n \leq \delta$$

$$= u_{zo} + \frac{\Delta \varphi}{2} \cdot (2x_n - \delta) \qquad \text{for } x_n > \delta \qquad \text{(B.24)}$$

where $u_{zo} = \dot{u}_{zo} \cdot t$ and $\Delta \varphi = \Delta \dot{\varphi} \cdot t$.

Inserting equations B.19–B.21 into B.13–B.18 results in:

$$\left.\begin{aligned}
\dot{\varepsilon}_{nn} &= \frac{\Delta \dot{u}_n}{\delta} + \frac{\Delta\dot{\varphi}\cdot x_z}{\delta}, && \text{(B.25)}\\
\dot{\varepsilon}_{ss} &= 0, && \text{(B.26)}\\
\dot{\varepsilon}_{zz} &= -\frac{\Delta \dot{u}_n}{\delta} - \frac{\Delta\dot{\varphi}\cdot x_z}{\delta} && \text{(B.27)}\\
\dot{\varepsilon}_{ns} &= \dot{\varepsilon}_{sn} = 1/2\,\frac{\Delta \dot{u}_s}{\delta} && \text{(B.28)}\\
\dot{\varepsilon}_{sz} &= \dot{\varepsilon}_{zs} = 0, && \text{(B.29)}\\
\dot{\varepsilon}_{zn} &= \dot{\varepsilon}_{nz} = 0. && \text{(B.30)}
\end{aligned}\right\} \text{ for } 0 \le x_n \le \delta$$

$$\dot{\varepsilon}_{ij} = 0 \qquad \text{for } x_n > \delta \qquad \text{(B.31)}$$

Combining equations B.25–B.31 with equations B.6–B.8 results in the strain-rate distribution assumed in the yield line (see equations B.2–B.5). The zone $0 \le x_n \le \delta$ can thus be considered as a yield zone.

B.2 *Yield line forces*

The yield line forces (generalized stresses) are by definition the stress-type variables $Q_1, Q_2, \ldots, Q_n$ that must be associated with the yield line deformation rates (generalized strain rates) $\dot{q}_1, \dot{q}_2, \ldots, \dot{q}_n$ in order that the rate of specific dissipation be given by:

$$W_s = Q_1 \cdot \dot{q}_1 + Q_2 \cdot \dot{q}_2 + \ldots + Q_n \cdot \dot{q}_n. \qquad \text{(B.32)}$$

In order to calculate the energy dissipated in plastic flow we have to evaluate the volume integral:

$$W_s = \int_V \sigma_{ij} \cdot \dot{\varepsilon}_{ij}\, dV. \qquad \text{(B.33)}$$

In the yield zone this integral reduces to:

$$W_s = \int_V (\sigma_{nn} \cdot \dot{\varepsilon}_{nn} + \sigma_{zz} \cdot \dot{\varepsilon}_{zz} + 2 \cdot \sigma_{ns} \cdot \dot{\varepsilon}_{ns})\, dV. \qquad \text{(B.34)}$$

For thin plates $\sigma_{zz} = 0$ so equation B.34 reduces to:

$$W_s = \int_V (\sigma_{nn} \cdot \dot{\varepsilon}_{nn} + 2 \cdot \sigma_{ns} \cdot \dot{\varepsilon}_{ns})\, dV. \qquad \text{(B.35)}$$

It should be noted that the choice of σ_{zz} has no influence on the energy dissipated in plastic flow, since the yield conditions are independent of hydrostatic stress. This can easily be seen by writing (Mase [10]):

$$W_s = \int_V \dot{\varepsilon}_{eq} \cdot f_y\, dV, \qquad \text{(B.36)}$$

where $\dot{\varepsilon}_{eq}$ is the equivalent or effective strain rate defined by:

$$\dot{\varepsilon}_{eq} = \sqrt{2/3 \cdot \dot{\varepsilon}_{ij} \cdot \dot{\varepsilon}_{ij}}. \tag{B.37}$$

Taking $\sigma_{zz} = 0$ therefore is not a static condition, as Out [15] wrote. A static condition would not be allowable in a kinematic approach.
Equation B.35 can be rewritten as follows:

$$W_s = \int_0^{\delta} dx_n \int_0^{l} dx_s \int_{-t_p/2}^{t_p/2} \left(\sigma_{nn} \cdot \left(\frac{\Delta \dot{u}_n}{\delta} + \frac{\Delta \dot{\varphi} \cdot x_z}{\delta} \right) + \cdot \sigma_{ns} \frac{\Delta \dot{u}_s}{\delta} \right) dx_z, \tag{B.38}$$

in which l is the length of the yield line.
This equation can be further simplified to get:

$$W_s = \int_0^{l} (\Delta \dot{\varphi} \cdot m + \Delta \dot{u}_n \cdot n + \Delta \dot{u}_s \cdot s) \, dx_s. \tag{B.39}$$

m, n and s are the bending moment, normal force and in-plane shear force per unit length, which can be calculated from the equations:

$$m = \int_{-t_p/2}^{t_p/2} \sigma_{nn} \cdot x_z \cdot dx_z, \tag{B.40}$$

$$n = \int_{-t_p/2}^{t_p/2} \sigma_{nn} \cdot dx_z, \tag{B.41}$$

$$s = \int_{-t_p/2}^{t_p/2} \sigma_{ns} \cdot dx_z, \tag{B.42}$$

B.3 *Validity of the derived formulas*

Both Dean [4] and Out [15, 16] did not discuss in detail the validity of generalized yield line theory. Dean stated that his mechanism solutions are valid only if the lateral deflection is so small that the approximation $\sin\theta = \theta$ is valid. He did not explain whether this restriction is caused by the approximations used in the kinematic equations or whether it is caused by the derivation of yield line deformation rates and yield line forces. Out [16] stated about the validity of generalized yield line theory: "Yield lines are simplifications of yield zones as they occur in reality. Full modeling of a yield zone could be done by using slip line theory, which implies that the geometry of the zone has to be modeled in detail. A yield line is two rather then three-dimensional. In other words, it is a local criterion. An error results from this reduction; for example energy dissipated at the boundary of deformed and undeformed sections is neglected (Drucker [5])." In the derivation of the yield line deformation rates it was assumed that in the yield zone $\dot{\varepsilon}_{zz} = -\dot{\varepsilon}_{nn}$. Since in the adjacent rigid plate elements $\dot{\varepsilon}_{zz} = 0$, this results in a mismatching (see Fig. 16). This mismatching becomes more pronounced with increasing generalized strain rates $\Delta \dot{u}_n$ and $\Delta \dot{\varphi}$ and decreasing width δ of the yield zone.

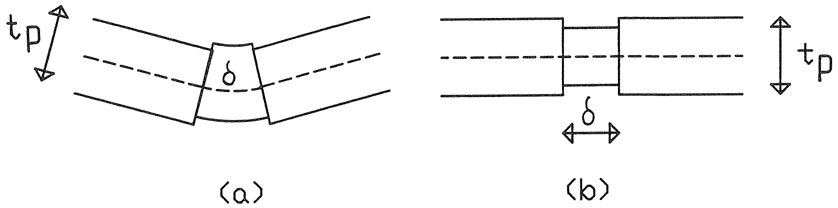

Fig. 16. Mismatching resulting from (a) bending and (b) stretching.

To analyze the validity of the derived formulas for the yield line deformation rates and the yield line forces the flow theory of plasticity is needed. Especially for large strains the flow theory of plasticity is most easily described using the Eulerian descriptive technique. For small strains (rotations and displacements may be large) the flow theory of plasticity can also be described using the Lagrangian description technique (see for instance Washizu [23] and Puthli [20]). If both the displacements and the displacements gradients are sufficiently small the Eulerian and the Lagrangian description may be taken as equal.
The derivation of the yield line deformation rates and yield line forces is based on a "small displacement" Lagrangian formulation. This means that the derivation is only valid for small displacement gradients, that is for

$$\frac{\partial a_i}{\partial x_j} \ll 1. \tag{B.43}$$

This is caused by the fact that the formula to calculate the strain rate from the velocity field

$$\dot{\varepsilon}_{ij} = 1/2 \cdot \left(\frac{\partial \dot{a}_i}{\partial x_j} + \frac{\partial \dot{a}_j}{\partial x_i} \right) \tag{B.44}$$

is valid only for small displacement gradients. For larger displacement gradients the formula:

$$\dot{\varepsilon}_{ij} = 1/2 \cdot \left(\delta_{kj} + \frac{\partial a_k}{\partial x_j} \right) \cdot \frac{\partial \dot{a}_k}{\partial x_i} + \left(\delta_{ki} + \frac{\partial a_k}{\partial x_i} \right) \cdot \frac{\partial \dot{a}_k}{\partial x_j} \tag{B.45}$$

should be used, where δ_{kj} is the Kronecker delta. In unabridged notation these equations for $\dot{\varepsilon}_{nn}$, $\dot{\varepsilon}_{zz}$ and $\dot{\varepsilon}_{ns}$ are:

$$\dot{\varepsilon}_{nn} = \left(1 + \frac{\partial a_n}{\partial x_n} \right) \cdot \frac{\partial \dot{a}_n}{\partial x_n} + \frac{\partial a_s}{\partial x_n} \cdot \frac{\partial \dot{a}_s}{\partial x_n} + \frac{\partial a_z}{\partial x_n} \cdot \frac{\partial \dot{a}_z}{\partial x_n}, \tag{B.46}$$

$$\dot{\varepsilon}_{zz} = \frac{\partial a_n}{\partial x_z} \cdot \frac{\partial \dot{a}_n}{\partial x_z} + \frac{\partial a_s}{\partial x_z} \cdot \frac{\partial \dot{a}_s}{\partial x_z} + \left(1 + \frac{\partial a_z}{\partial x_z} \right) \cdot \frac{\partial \dot{a}_z}{\partial x_z}, \tag{B.47}$$

$$\dot{\varepsilon}_{ns} = 1/2 \cdot \left(\frac{\partial \dot{a}_n}{\partial x_s} + \frac{\partial \dot{a}_s}{\partial x_n} \right) + 1/2 \cdot \left(\frac{\partial a_n}{\partial x_s} \cdot \frac{\partial \dot{a}_n}{\partial x_n} + \frac{\partial a_n}{\partial x_n} \cdot \frac{\partial \dot{a}_n}{\partial x_s} \right) +$$

$$+ 1/2 \cdot \left(\frac{\partial a_s}{\partial x_s} \cdot \frac{\partial \dot{a}_s}{\partial x_n} + \frac{\partial a_s}{\partial x_n} \cdot \frac{\partial \dot{a}_s}{\partial x_s} \right) + 1/2 \cdot \left(\frac{\partial a_z}{\partial x_s} \cdot \frac{\partial \dot{a}_z}{\partial x_n} + \frac{\partial a_z}{\partial x_n} \cdot \frac{\partial \dot{a}_z}{\partial x_z} \right). \qquad \text{(B.48)}$$

As a result generalized yield line theory is valid only for small displacement gradients. From the equations B.22–B.24 for the displacement field it can be concluded that the theory is valid only if:

$$\frac{\partial u_n}{\partial x_n} \ll 1 \rightarrow \frac{\Delta u_n}{\delta} \ll 1 \qquad \text{(B.49)}$$

$$\frac{\partial u_s}{\partial x_n} \ll 1 \rightarrow \frac{\Delta u_s}{\delta} \ll 1 \qquad \text{for } 0 \leq x_n < \delta \qquad \text{(B.50)}$$

$$\frac{\partial u_z}{\partial x_z} \ll 1 \rightarrow \frac{\Delta \varphi \cdot x_n}{\delta} \ll 1 \rightarrow \Delta \varphi \ll 1 \qquad \text{(B.51)}$$

Thus normal and in-plane shear yield line deformations should be very small compared to the width of the yield zone and the rotational deformation in the yield line should be much smaller than 1 rad, that is much smaller than 57°. Also it can be seen that in a yield zone where normal and in-plane shear deformations occur, the width of the yield zone cannot be equal to zero. This can also be concluded from the equations for the displacement field, since a yield zone width δ equal to zero would result in a discontinuous displacement field and hence in rupture of the material.

The restriction that generalized yield line theory is valid only for small displacements gradients can be made plausible by looking in more detail at a yield line with only normal deformation. In the Eulerian description equation B.44 is exact for displacement gradients of any magnitude. But in the Eulerian description the stresses have to be integrated over the instantaneous thickness $t_p(t)$ of the plate (and not over the initial thickness t_p of the plate, as in the Lagrangian description) to obtain the generalized stresses. Let l be the length of the yield line (which is kept constant during deformation), t_p and $t_p(t)$ the initial and actual thickness of the plate respectively, and δ and $\delta(t)$ the initial and actual width of the yield zone respectively, with $\delta(t) = \delta + \Delta u_n$. From global volume invariance it can be concluded that

$$t_p(t) = \frac{\delta}{\delta(t)} \cdot t_p = \frac{\delta}{\delta + \Delta u_n} \cdot t_p. \qquad \text{(B.52)}$$

This implies that using equation B.44 to calculate the strain rate field from the velocity field the Eulerian and the Lagrangian approach will only give the same result if $t_p(t) \simeq t_p$, that is if $\Delta u_n \ll \delta$. The change of thickness in a yield line with normal deformations is not imaginary. Kachanov [8] described that a jump in the normal component of velocity leads to abrupt thickening or thinning of the plate along the line of discontinuity. This line is a mathematical idealization of the local development of a "neck" which is observed in experiments (see Fig. 17).

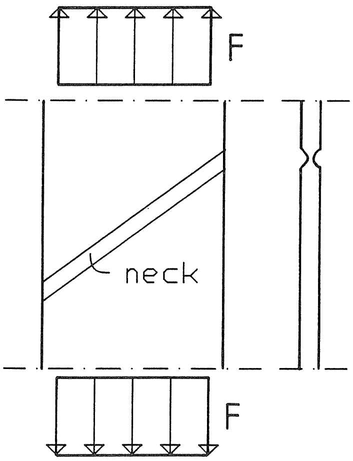

Fig. 17. A neck observed in a tensile test on a strip.

The limitations for the derived formulas expressed by equations B.49–B.51 are not valid for yield lines in which only bending moments or only shear forces are active. Hill [6] described a general theory of sheet-bending using cylindrical coordinates and an Eulerian description. He showed that for a sheet bent in plane strain (negligible strain in the width direction) the plastic work done per unit width equals $m_p \cdot L \cdot \alpha$, where L is the original length of the sheet, α is the angle of bending per unit original length, and $m_p = 1/4 \cdot t_p^2 \cdot 2/\sqrt{3} \cdot f_y$. This derivation is valid for strains of any magnitude. We can therefore conclude that the rate of energy dissipated in yield lines with only bending moments acting in them can always be calculated by:

$$\dot{W} = m_p \cdot \Delta\dot{\varphi} \cdot l, \tag{B.53}$$

where $\Delta\varphi = \alpha \cdot \delta$, δ is the width of the yield zone, and l is the length of the yield zone, regardless of the magnitude of $\Delta\varphi$. It should be kept in mind however that when a large rotational deformation $\Delta\varphi$ is concentrated in a small yield zone width δ, a large mismatching results.

For a yield line with only shear forces active, equations B.44 and B.45 result in the same strain rate field, namely:

$$\dot{\varepsilon}_{nn} = \dot{\varepsilon}_{ss} = \dot{\varepsilon}_{zz} = \dot{\varepsilon}_{sz} = \dot{\varepsilon}_{nz} = 0, \tag{B.54}$$

$$\dot{\varepsilon}_{ns} = 1/2 \cdot \Delta\dot{u}_s/\delta \tag{B.55}$$

Therefore for yield lines with only shear forces active in them the restriction $\Delta u_s/\delta \ll 1$ does not apply. Also, a shear yield line does not cause any mismatching, no matter how small the width of the yield zone.

It is concluded that the validity of generalized yield line is subject to the following restrictions:

1. For yield lines with bending moment, normal and in-plane shear forces:

$$\Delta\varphi \ll 1 \text{ [rad]}, \quad \Delta u_n \ll \delta \quad \text{and} \quad \Delta u_s \ll \delta \tag{B.56}$$

2. For yield lines with only a normal force:

$$\Delta u_n \ll \delta \tag{B.57}$$

3. For yield lines with only a bending moment: no restrictions, but concentrating a large rotation in a small yield zone results in a large mismatching.
4. For yield lines with only an in-plane shear force: no restrictions.

In generalized yield line theory the width δ of the yield zone is a fictitious quantity. Its magnitude is undetermined. One might conclude therefore that the restrictions $\Delta u_n \ll \delta$ and $\Delta u_s \ll \delta$ have no practical importance because the limitations on the normal deformation Δu_n and the in-plane shear deformation Δu_s can be eliminated by assuming a large width of the yield zone. It must be noted however that in the derivation of the kinematic equations of a yield line mechanism the assumption is made that the width of the yield zone is so small (compared to the width of the rigid plate elements) that the yield zones may be considered as yield lines.

Appendix C: Examples of the work method

C.1 *A simple true mechanism*

In this section the equilibrium mechanism solution and a non-equilibrium mechanism solution for a simple true mechanism with only one yield line will be described. Therefore an axially loaded panel as shown in Fig. 18 is considered. First the equilibrium mechanism solution is given. The collapse load corresponding to this mechanism will be denoted by F_{eq}.

The equilibrium mechanism solution

The mechanism of the axially loaded panel is determined by the yield line pattern (in this case one yield line) and the velocities of the rigid plane element. The velocities are described by the parameters $\dot{\theta}$ and $\dot{a}$, where $\dot{\theta}$ is the rotational velocity of the plane element around the yield line, and $\dot{a}$ the in-plane velocity normal to the yield line. Choosing θ and $\dot{\theta}$ as deformation and deformation rate parameter, we have:

$$\theta(t) = \dot{\theta} \cdot t, \tag{C.1}$$

where t denotes time. The yield line deformations and deformations rates, as well as the out of plane deflection w, out of plane deflection rate $\dot{w}$, end displacement v and end velocity $\dot{v}$ (see Fig. 18), can be determined from the velocities and instantaneous positions of the rigid plate elements. The kinematic equations are thus given by:

$$\Delta\varphi = \theta, \qquad \Delta\dot{\varphi} = \dot{\theta}, \tag{C.2}$$

$$\Delta u_n = a, \qquad \Delta\dot{u}_n = \dot{a}, \tag{C.3}$$

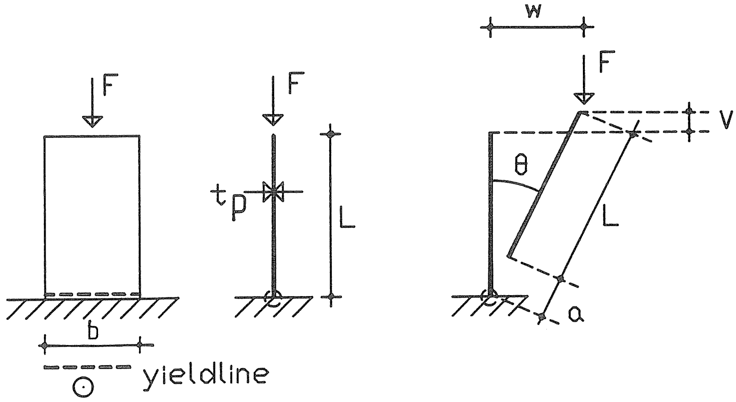

Fig. 18. A simple true mechanism.

$$\Delta u_s = 0 \qquad \Delta \dot{u}_s = 0, \tag{C.4}$$

$$v \quad = L - (L + a) \cdot \cos\theta, \qquad \dot{v} \quad = (L + a) \cdot \sin\theta \cdot \dot{\theta} - \dot{a} \cdot \cos\theta, \tag{C.5}$$

$$w \quad = (L + a) \cdot \sin\theta, \qquad \dot{w} \quad = (L + a) \cdot \cos\theta \cdot \dot{\theta} + \dot{a} \cdot \sin\theta. \tag{C.6}$$

Since no shear forces are active in the yield line, the yield condition in generalized stress space is expressed by (see Appendix A):

$$\psi = \frac{\Delta\dot{\varphi}}{|\Delta\dot{\varphi}|} \cdot \frac{m}{m_p} + \left(\frac{n}{n_p}\right)^2 - 1 = 0. \tag{C.7}$$

Applying the normality rule to this surface results in:

$$\Delta\dot{u}_n / \Delta\dot{\varphi} = 2 \cdot m_p / n_p \cdot n / n_p \cdot \frac{\Delta\dot{\varphi}}{|\Delta\dot{\varphi}|} = \dot{a} / \dot{\theta} \tag{C.8}$$

Equating the rate of external work to the rate of internal plastic work at the yield lines we find:

$$m \cdot b \cdot \Delta\dot{\varphi} + n \cdot b \cdot \Delta\dot{u}_n = F_{eq} \cdot \dot{v}. \tag{C.9}$$

Assuming:

$$n = \alpha \cdot n_p, \tag{C.10}$$

and inserting the kinematic equations, the yield condition and the flow rule into equation C.9 results in:

$$\frac{F_{eq}}{b \cdot n_p} = \frac{(1 + \alpha^2)}{(L + a) \cdot \sin\theta \cdot n_p / m_p - 2 \cdot \alpha \cdot \cos\theta}. \tag{C.11}$$

Since $a \ll L$, only a small error is made if equation C.11 is replaced by:

$$\frac{F_{eq}}{b \cdot n_p} = \frac{(1 + \alpha^2)}{L \cdot \sin\theta \cdot n_p/m_p - 2 \cdot \alpha \cdot \cos\theta}. \tag{C.12}$$

In order to find the smallest upper bound the ratio $F_{eq}/(b \cdot n_p)$ is minimized with respect to α. Taking:

$$A = \cos^2\theta, \tag{C.13}$$

and

$$B = L \cdot \sin\theta \cdot n_p/m_p, \tag{C.14}$$

results in:

$$\alpha = \frac{+B - \sqrt{B^2 + 4 \cdot A}}{2 \cdot \sqrt{A}}. \tag{C.15}$$

So the limit load F_{eq} can be calculated for every deformation state, characterized by the parameter θ, from the equation:

$$\frac{F_{eq}}{b \cdot n_p} = \frac{-B + \sqrt{B^2 + 4 \cdot A}}{2 \cdot A}. \tag{C.16}$$

From equations C.15 and C.16 it can be concluded that:

$$\alpha = \frac{n}{n_p} = -\frac{F_{eq}}{b \cdot n_p} \cdot \cos\theta. \tag{C.17}$$

This is exactly the condition for in-plane equilibrium. The lowest upper bound is thus found when the in-plane equilibrium is satisfied.
The same solution can be found by deriving the equilibrium equations from the principle of virtual work. Substituting equations C.2, C.3 and C.5 into equation C.9 one finds:

$$m \cdot b \cdot \theta + n \cdot b \cdot \dot{a} = F_{eq} \cdot (L + a) \cdot \sin\theta \cdot \dot{\theta} - F_{eq} \cdot \dot{a} \cdot \cos\theta. \tag{C.18}$$

Since $\dot{a}$ and $\dot{\theta}$ are independent it can be concluded that:

$$n \cdot b \cdot \dot{a} = -F_{eq} \cdot \dot{a} \cdot \cos\theta, \tag{C.19}$$

and

$$m \cdot b \cdot \dot{\theta} = F_{eq} \cdot (L + a) \cdot \sin\theta \cdot \theta. \tag{C.20}$$

From equations C.19 and C.20 the ratios n/n_p and m/m_p can be derived:

$$\frac{n}{n_p} = \frac{-F_{eq}}{b \cdot n_p} \cdot \cos\theta, \tag{C.21}$$

and

$$\frac{m}{m_p} = \frac{F_{eq}}{b \cdot n_p} \cdot (L + a) \cdot \sin\theta \cdot n_p/m_p. \tag{C.22}$$

Combining equations C.21 and C.22 with equation C.7 and replacing $(L+a)$ by L results in:

$$\left(\frac{F_{eq}}{b \cdot n_p}\right)^2 \cdot \cos^2\theta + \frac{F_{eq}}{b \cdot n_p} \cdot L \cdot \sin\theta \cdot n_p/m_p - 1 = 0. \tag{C.23}$$

Taking $A = \cos^2\theta$ and $B = L \cdot \sin\theta \cdot n_p/m_p$ (compare C.13 and C.14) results in equation C.16.

From equations C.21 and C.23 the ratio n/n_p can be determined as a function of θ and hence the ratio $\dot{a}/\dot{\theta}$ as a function of θ (see equation C.8). The corresponding a can then be calculated by evaluating the integral:

$$\int_0^t \dot{a} \cdot dt = \int_0^\theta \dot{a}/\dot{\theta} \cdot d\theta. \tag{C.24}$$

The corresponding v and w can be calculated from equations C.5, and C.6, or may be approximated by the equations:

$$v = L - L \cdot \cos\theta, \tag{C.25}$$

$$w = L \cdot \sin\theta. \tag{C.26}$$

In the above mechanism the in-plane equilibrium of the rigid plane elements is satisfied. In this very simple example the in-plane equilibrium has to be considered in only one direction. In general however one has to consider three directions, namely two in-plane translations and one in-plane rotation.

A non-equilibrium mechanism solution

In this section two non-equilibrium mechanism solutions will be described, one with only bending moments active in the yield line and one with ony normal forces active in the yield line. The collapse load corresponding to these mechanisms is denoted by F_{neq}.

First the mechanism solution with only bending moments active in the yield line will be described.

Considering once more the plate of Fig. 18, now the assumption $\dot{a} = 0$ is made, so that the velocities of the plane elements are described by only one parameter. Equations C.2 to C.6 then reduce to:

$$\Delta\varphi = \theta, \qquad \Delta\dot{\varphi} = \dot{\theta}, \tag{C.27}$$

$$\Delta u_n = \Delta u_s = 0, \qquad \Delta\dot{u}_n = \Delta\dot{u}_s = 0, \tag{C.28}$$

$$v = L - L \cdot \cos\theta, \qquad \dot{v} = L \cdot \sin\theta \cdot \dot{\theta}, \tag{C.29}$$

$$w = L \cdot \sin\theta, \qquad \dot{w} = L \cdot \cos\theta \cdot \dot{\theta}. \tag{C.30}$$

Analogous to the first problem one obtains:

$$\frac{F_{neq}}{b \cdot n_p} = \frac{1}{B} = \frac{1}{L \cdot \sin\theta \cdot n_p/m_p}. \tag{C.31}$$

The corresponding v and w can be calculated from equations C.29 and C.30.
From equation C.31 it can be seen that very small values of θ result in very large values of F_{neq}. A bound on F_{neq} for very small θ is given by another mechanism, namely the mechanism in which only normal forces are active in the yield line. To define this mechanism it is assumed that $\dot{\theta}=0$. This results in:

$$\frac{F_{\mathrm{neq}}}{b \cdot n_{\mathrm{p}}}=1. \qquad \text{(C.32)}$$

The mechanisms governs for $B<1$.

C.2 *A simple quasi mechanism*

In this section the equilibrium mechanism solution and a non-equilibrium mechanism solution for a simple quasi mechanism are described. Therefore a laterally loaded panel with two restrained built-in edges and two free edges, as shown in Fig. 19 is considered. First the equilibrium mechanism solution will be described. The collapse load corresponding to this mechanism is denoted by F_{eq}.

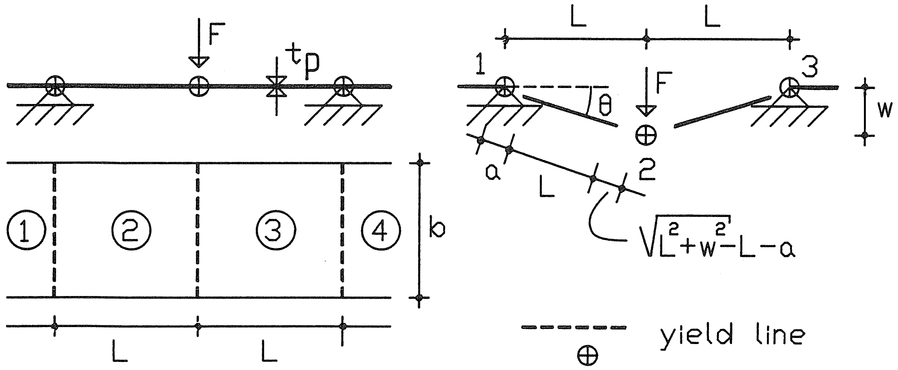

Fig. 19. A simple quasi mechanism.

The equilibrium mechanism solution

The mechanism is determined by three yield lines and the velocities and instantaneous positions of the thus defined four rigid plane elements. The boundary conditons require that the rigid plane elements 1 and 4 do not experience in-plane translations. The velocities of the plane elements 2 and 3 are described by the parameters $\dot{\theta}_2$, $\dot{a}_2$, $\dot{\theta}_3$ and $\dot{a}_3$, where $\dot{a}_2$ and $\dot{a}_3$ are the in-plane velocities normal to the yield lines, and $\dot{\theta}_2$ and $\dot{\theta}_3$ the rotational velocities around yield lines 1 and 3, respectively. For reasons of symmetry we have:

$$\dot{a}_2=\dot{a}_3=\dot{a}, \qquad \text{(C.33)}$$

$$\dot{\theta}_2=\dot{\theta}_3=\dot{\theta}. \qquad \text{(C.34)}$$

This results in the following yield line deformations and deformation rates:

$$\Delta\varphi_1 = \Delta\varphi_3 = -\theta, \qquad \Delta\dot{\varphi}_1 = \Delta\dot{\varphi}_3 = -\dot{\theta}, \tag{C.35}$$

$$\Delta\varphi_2 = 2\cdot\theta, \qquad \Delta\dot{\varphi}_2 = 2\cdot\dot{\theta}, \tag{C.36}$$

$$\Delta u_{n1} = \Delta u_{n3} = a, \qquad \Delta\dot{u}_{n1} = \Delta\dot{u}_{n3} = \dot{a}, \tag{C.37}$$

$$\Delta u_{n2} = 2\cdot(L/\cos\theta - L - a) \qquad \Delta\dot{u}_{n2} = 2\cdot(L/\cos^2\sin\theta\cdot\dot{\theta} - \dot{a}), \tag{C.38}$$

$$w = L\cdot\tan\theta, \qquad \dot{w} = L/\cos^2\theta\cdot\dot{\theta}. \tag{C.39}$$

In the yield lines only bending moments and normal forces are active. The yield condition in generalized stress space is thus expressed by (see Appendix A):

$$\psi = \frac{\Delta\dot{\varphi}}{|\Delta\dot{\varphi}|}\cdot\frac{m}{m_\mathrm{p}} + \left(\frac{n}{n_\mathrm{p}}\right)^2 - 1 = 0. \tag{C.40}$$

Applying the normality rule to this yield surface results in:

$$n/n_\mathrm{p} = 1/2\cdot n_\mathrm{p}/m_\mathrm{p}\cdot\Delta\dot{u}_\mathrm{n}/|\Delta\dot{\varphi}| = 2/t_\mathrm{p}\cdot\Delta\dot{u}_\mathrm{n}/|\Delta\dot{\varphi}|. \tag{C.41}$$

Since n cannot become larger than n_p, we have:

$$n/n_\mathrm{p} = 1 \quad \text{for} \quad 2/t_\mathrm{p}\cdot\Delta\dot{u}_\mathrm{n}/|\Delta\dot{\varphi}| > 1. \tag{C.42}$$

The equilibrium equations result from the notion that the work rate by the external forces is equal to the rate of energy dissipated in plastic flow, so:

$$2\cdot b\cdot(m_1\cdot\dot{\theta} + n_1\cdot\dot{a} + m_2\cdot\dot{\theta} + n_2\cdot(L/\cos^2\theta\cdot\sin\theta\cdot\dot{\theta} - \dot{a})) = F_\mathrm{eq}\cdot L/\cos^2\theta\cdot\dot{\theta}. \tag{C.43}$$

Since $\dot{a}$ and $\dot{\theta}$ are independent, it can be concluded that:

$$n_1 = n_2 = n_3, \qquad \text{(and therefore } m_1 = -m_2 = m_3) \tag{C.44}$$

and

$$\frac{F_\mathrm{eq}}{b\cdot n_\mathrm{p}} = t_\mathrm{p}/L\cdot\cos^2\theta\cdot m_1/m_\mathrm{p} + 2\cdot\sin\theta\cdot n_1/n_\mathrm{p}. \tag{C.45}$$

Combining equations C.35 to C.39 with C.41 and C.44 results in:

$$\dot{a} = 1/2\cdot L\cdot\sin\theta/\cos^2\theta\cdot\dot{\theta}, \tag{C.46}$$

and

$$\frac{n_1}{n_\mathrm{p}} = \frac{n_2}{n_\mathrm{p}} = \frac{n_3}{n_\mathrm{p}} = L/t_\mathrm{p}\cdot\sin\theta/\cos^2\theta \quad \text{for} \quad 0 \leq L/t_\mathrm{p}\cdot\sin\theta/\cos^2\theta \leq 1, \tag{C.47}$$

$$\frac{n_1}{n_\mathrm{p}} = \frac{n_2}{n_\mathrm{p}} = \frac{n_3}{n_\mathrm{p}} = 1 \qquad \text{for} \quad L/t_\mathrm{p}\cdot\sin\theta/\cos^2\theta > 1. \tag{C.48}$$

Substituting equations C.47, C.48 and C.40 into C.45 one finds:

$$\frac{F_{eq}}{b \cdot n_p} = t_p/L \cdot \cos^2 \theta + L/t_p \cdot \sin^2 \theta / \cos^2 \theta \quad \text{for} \quad 0 \leq L/t_p \cdot \sin \theta / \cos^2 \theta \leq 1, \tag{C.49}$$

$$\frac{F_{eq}}{b \cdot n_p} = 2 \cdot \sin \theta \quad \text{for} \quad L/t_p \cdot \sin \theta / \cos^2 \theta \geq 1. \tag{C.50}$$

In the above mechanism the in-plane equilibrium of the rigid plane elements is satisfied. Next a non-equilibrium mechanism solution will be described for which this is not the case. The collapse load corresponding to this mechanism will be denoted by F_{neq}.

A non-equilibrium solution

Considering once more the plate of Fig. 19, the assumption $\dot{a} = 0$ is made, so that the velocities of the plane elements are described by the parameters θ and $\dot{\theta}$ only. Analogous to the equilibrium mechanism, one finds:

$$\frac{F_{neq}}{b \cdot n_p} = t_p/L \cdot \cos^2 \theta + 2 \cdot L/t_p \cdot \sin^2 \theta / \cos^2 \theta \quad \text{for} \quad 0 \leq L/t_p \cdot \sin \theta / \cos^2 \theta \leq 1/2, \tag{C.51}$$

$$\frac{F_{neq}}{b \cdot n_p} = 2 \cdot \sin \theta \quad \text{for} \quad L/t_p \cdot \sin \theta / \cos^2 \theta \geq 1/2. \tag{C.52}$$

Appendix D: An example of the determination of a non-equilibrium mechanism

In this appendix a non-equilibrium mechanism for an in-plane loaded square plate is described (see Fig. 20). It is shown how the instantaneous positions and velocities of the vertices of the rigid plane elements can be determined as a function of one deformation and one deformation rate parameter. From these instantaneous positions and velocities the yield line deformations and deformation rates can be determined as explained in section 5.3.

The mechanism is determined by the cross-shaped yield line pattern and the velocities of the thus defined four rigid plane elements. The out of plane deflection w and the out of plane deflection rate $\dot{w}$ are chosen as deformation and deformation rate parameters. Assuming that the initially coinciding vertices of plane element 1 and 3 remain linked during deformation, and considering the boundary conditions of the plane elements, the velocities and instantaneous positions of the vertices of the rigid plane elements can be expressed as a function of the parameters w and $\dot{w}$ only. For reasons of symmetry only one quarter of the plate needs to be considered (see Fig. 21).

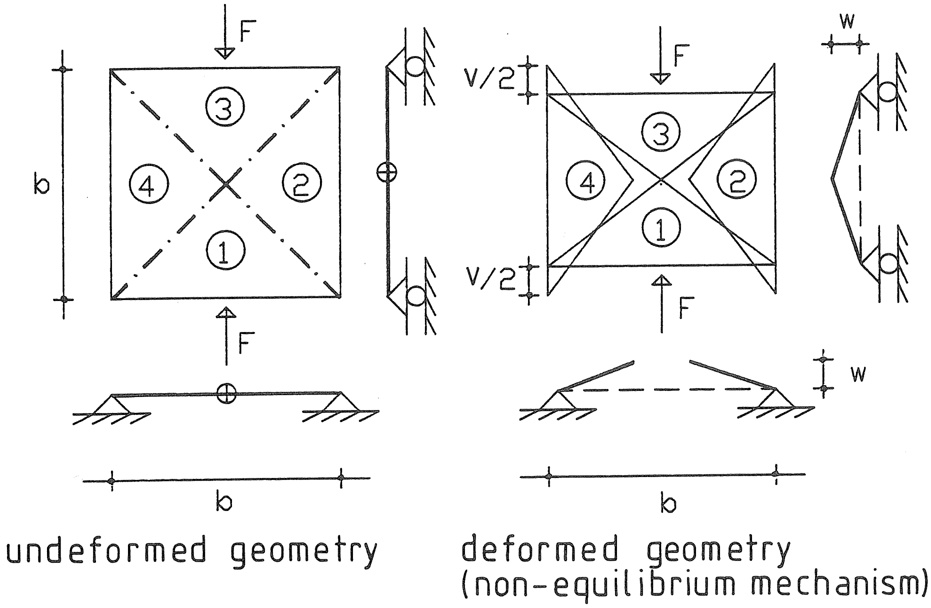

Fig. 20. Geometry of a non-equilibrium mechanism for an in-plane loaded square plate.

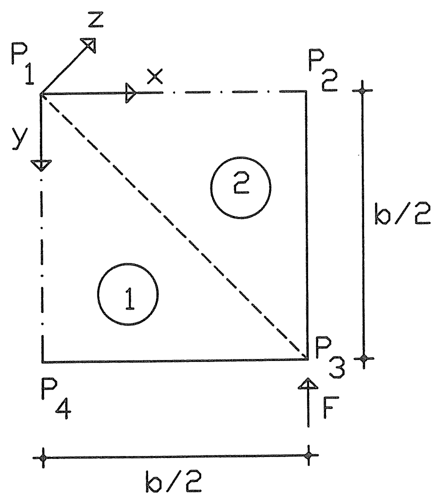

Fig. 21. For reasons of symmetry only one quarter of the plate needs to be considered.

The initial coordinates of the vortices of the rigid plane elements are given by:

$$P_1(0) = (0, 0, 0) \quad \text{(D.1)}$$

$$P_2(0) = (b/2, 0, 0) \quad \text{(D.2)}$$

$$P_3(0) = (b/2, b/2, 0) \quad \text{(D.3)}$$

$$P_4(0) = (0, b/2, 0) \quad \text{(D.4)}$$

The initial end points of yield line 1 are the points P_1 and P_3.
The instantaneous coordinates of the vertices of rigid plane element 1 are given by:

$$P_{1,\mathrm{e}1}(w) = (0, 0, w) \quad \text{(D.5)}$$

$$P_{3,\mathrm{e}1}(w) = (b/2, \sqrt{(b/2)^2 - w^2}, 0) \quad \text{(D.6)}$$

$$P_{4,\mathrm{e}1}(w) = (0, \sqrt{(b/2)^2 - w^2}, 0) \quad \text{(D.7)}$$

The instantaneous coordinates of the vertices of rigid plane element 2 are given by:

$$P_{1,\mathrm{e}2}(w) = (b/2)/\sqrt{(b/2)^2 + w^2} \cdot (-\, b/2, 0, w) + (b/2, 0, 0) \quad \text{(D.8)}$$

$$P_{2,\mathrm{e}2}(w) = (b/2, 0, 0) \quad \text{(D.9)}$$

$$P_{3,\mathrm{e}2}(w) = (b/2, 0, 0) \quad \text{(D.10)}$$

Finally, the instantaneous coordinates of the end points of the yield line are given by:

$$P_{1,\mathrm{y}}(w) = (0, 0, w) \quad \text{(D.11)}$$

$$P_{3,\mathrm{y}}(w) = (b/2, \sqrt{(b/2)^2 - w^2}, 0) \quad \text{(D.12)}$$

The velocity of the vertices of the plane elements can be calculated by differentiating the instantaneous coordinates with respect to w. Thus the velocities of the vertices of plane element 1 are given by:

$$\dot{P}_{2,\mathrm{e}1}(w) = (0, 0, 1) \cdot \dot{w} \quad \text{(D.13)}$$

$$\dot{P}_{3,\mathrm{e}1}(w) = (0, w/\sqrt{(b/2)^2 - w^2}, 0) \cdot \dot{w} \quad \text{(D.14)}$$

$$\dot{P}_{4,\mathrm{e}1}(w) = (0, w/\sqrt{(b/2)^2 - w^2}, 0) \cdot \dot{w} \quad \text{(D.15)}$$

The velocities of the vertices of plane element 2 are given by:

$$\dot{P}_{1,\mathrm{e}2}(w) = -\, w \cdot (b/2)/\sqrt{((b/2)^2 + w^2)^3} \cdot (-\, b/2, 0, w) \cdot \dot{w} + (b/2)/\sqrt{(b/2)^2 + w^2} \cdot (0, 0, 1) \cdot \dot{w} \quad \text{(D.16)}$$

$$\dot{P}_{2,\mathrm{e}2}(w) = (0, 0, 0) \cdot \dot{w} \quad \text{(D.17)}$$

$$\dot{P}_{3,\mathrm{e}2}(w) = (0, 0, 0) \cdot \dot{w} \quad \text{(D.18)}$$

Finally, the velocities of the end points of the yield line are given by:

$$\dot{P}_{1,\mathrm{y}} = (0, 0, 1) \cdot \dot{w} \quad \text{(D.19)}$$

$$\dot{P}_{3,y} = (0, w/\sqrt{(b/2)^2 - w^2}, 0) \cdot \dot{w} \tag{D.19}$$

The in-plane displacement v of the loaded plate edge with respect to the plate center can be calculated from:

$$v = b/2 - \sqrt{(b/2)^2 + w^2}. \tag{D.20}$$

The in-plane displacement rate $\dot{v}$ is given by:

$$\dot{v} = w/\sqrt{(b/2)^2 + w^2} \cdot \dot{w} \tag{D.21}$$